Thermal chamber for adhesives testing machines

Artur Jorge Morais Louçano

Master dissertation thesis

Supervisor: Prof. António Mendes Lopes

Co-supervisor: Inv. Carlos Moreira da Silva

Co-supervisor: Prof. Lucas F. M. da Silva

Integrated Master in Mechanical Engineering

Automation option

July 2017

Abstract

Adhesives are materials increasingly used in the industry, so the knowledge of their properties is important at an engineering level. FEUP adhesives group (ADFEUP) is a group that is focused on testing and evaluating adhesive's properties. Two of the machines that exist in the ADFEUP laboratory are the glass transition temperature machine and the torsion machine for determining adhesive shear properties.

The purpose of this work is to design a portable thermal chamber to be used with the two machines for testing adhesives at different temperatures. The chamber needs to be capable of testing adhesives in a temperature range from -100 to 200 °C.

The design of the thermal chamber was done taking in consideration the requirements of the system. For the validation of the design, a thermal and flow simulations were carried out using SolidWorks software.

For the glass transition temperature machine, simulations of the temperature distribution in the adhesive were performed, since in this test the heating/cooling rate must be fast, but at the same time the temperature gradient the adhesive must be small.

Finally, the automation project was executed. The electronic components were selected and the electric circuit was done.

Câmara térmica para máquinas de ensaios de adesivos

Resumo

Os adesivos são materiais que têm vindo a ser cada vez mais utilizados na indústria, por isso o conhecimento das suas propriedades é importante a nível de projetos de engenharia. O grupo de adesivos da FEUP (ADFEUP) é um grupo de investigação que se foca em testar e avaliar as propriedades dos adesivos. Duas das máquinas existente no laboratório do ADFEUP são a máquina para determinação da temperatura de transição vítrea dos adesivos e a máquina de torção para determinar as propriedades dos adesivos ao corte.

O objetivo deste trabalho é desenvolver uma câmara térmica portátil que seja capaz de testar adesivos nestas duas máquinas. A câmara tem de ser capaz de testar adesivos numa gama de temperaturas entre os -100 e os 200 °C.

O projeto da câmara térmica foi feito tendo em consideração os requisitos do sistema. Para validar o projeto desenvolvido, foram realizadas simulações térmicas e de movimento de fluidos, através do *software* SolidWorks.

Para a máquina de determinação da temperatura de transição vítrea de adesivos, foram efetuadas simulações da distribuição de temperaturas ao longo do adesivo, uma vez que nestes testes a velocidade de aquecimento/arrefecimento tem que ser muito rápida e ao mesmo tempo o gradiente de temperaturas no adesivo tem que ser baixo.

Finalmente, foi concretizado o projeto de automação. Para tal, foram selecionados os componentes eletrónicos e foi projetado o circuito elétrico.

Acknowledgments

I would like to express my gratitude to my supervisor Professor António Mendes Lopes, for all the patience and availability during the dissertation, and for helping me in the automation project of the system.

I would like to thank my co-supervisor Inv. Carlos Moreira da Silva, for all the availability and for helping me in the design of the thermal chamber.

I would also like to thank my co-supervisor Prof. Lucas F. M. da Silva, for all the availability and support during the development of the dissertation.

To all my colleagues in the Adhesive Group, for their friendship, help, and availability;

To all my friends that helped me and supported me in the hardest times;

To my family for all the support and encouragement, I am profoundly grateful.

Contents

List of figures

List of Tables

1 Introduction

1.1 Background and motivation

Traditional structural bonds are usually done by welding, screwing or riveting. However, adhesives have been more and more used and asserting themselves as a viable alternative to these traditional methods. This is because adhesives have several advantages, such as a uniform stress distribution through the joint, the ability to resist bending and vibration, and the capacity to connect a wide range of materials.

To allow a correct use of adhesives as structural bonds in engineering design, it becomes important to understand well their properties. Adhesives are very sensitive to temperature, so the glass transition temperature, *Tg*, of adhesives is an important property to know since it is normally close to the ambient temperature, or the operating temperature. The knowledge of the glass transition temperature is very important to structural bonds because below this temperature the adhesive has a hard glass state behavior and above this temperature, the adhesive has a rubber-like behavior, losing its structural capabilities. Another important property is the adhesive's behavior to shear stress. This property is very important because in real case applications, the shear stress is the most common stress applied to the adhesive.

Because of the importance of those properties and the knowledge of them, two machines were developed previously at the FEUP adhesives group (ADFEUP). These machines reside in the ADFEUP laboratory. One is a machine for determining the glass transition temperature, Figure 1.1. The other is a torsion machine that has the function of testing adhesive joints behavior to shear stress, Figure 1.2.

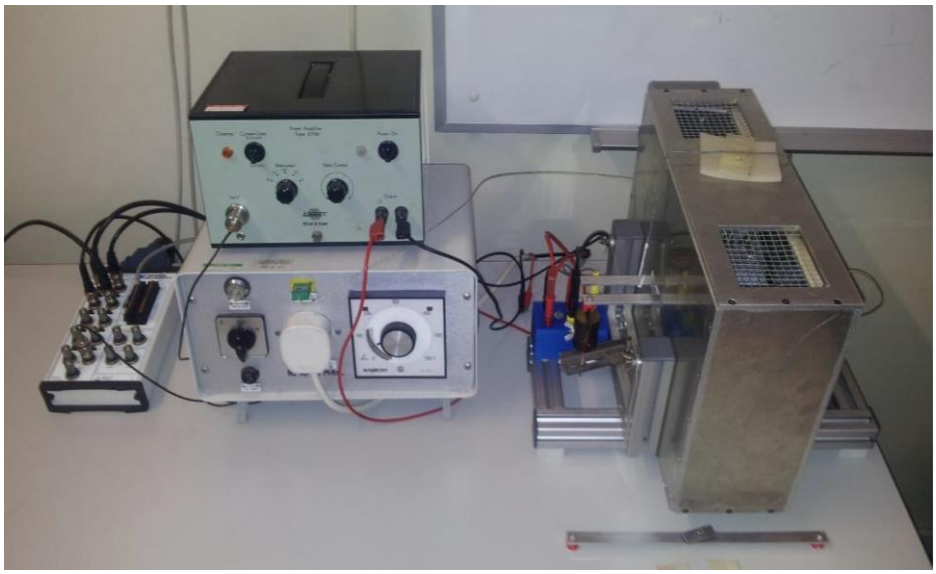

Figure 1.1 - Machine that determines glass transition temperature of adhesives, *Tg*.

Figure 1.2 - Torsion machine that determines adhesive shear properties.

The *Tg* machine is fully functional and already has a thermal chamber to vary the temperature. However, the chamber only allows a semi-automatic heating process of the specimen under

test, which limitates the accuracy of the results. The torsion machine is also functional, but operates only at ambient temperature, since it has no thermal chamber yet.

It is then necessary the implementation of a thermal chamber, that allows the test of adhesives in a fully automatic way, so that it is possible to improve the determination of the *Tg* and allow the test of adhesives at different temperatures in the torsion machine. It is also required that the thermal chamber can operate at negative temperatures, for testing adhesives for cryogenic applications.

1.2 Objectives

The main goal of this thesis is the development of a portable thermal chamber for the glass transition temperature machine, so that the determination of the *Tg* can be improved, and for the torsion machine, to test adhesives at different temperatures.

The development of this thesis is based on the following objectives:

- Design of a portable thermal chamber that can operate between the temperature range of -100 to 200 °C. The chamber needs to have a fast response, so that the determination of the glass transition temperature can be the most accurate possible;
- Perform the mechanical and thermal design of the thermal chamber, so that it can comply the requirements of the system;
- Carry out the automation project of the chamber, so that the temperature control is fully automatic. The system must perform the tests automatically, being only necessary to define the target temperature and the heating/cooling rate required for the test.

1.3 Methodology

The first stage of the dissertation was a literature review to understand how the glass transition temperature machine and the torsion machine work. It was also made a review about the typical thermal chambers and about cooling/heating systems.

After the review, considering the requirements for the thermal machine and how thermal machines are usually made, the design of the chamber was done. To validate the design, thermal and flow simulations were done, analyzing the temperature distribution in the chamber and in the adhesive, and analyzing the heating/cooling velocity of the tests.

Finally, the automation project was done. All the electronic/electric components were selected and the electric circuit of the system was done.

1.4 Plan of the thesis

This dissertation is divided into six chapters that describe the design and development of the thermal chamber.

In the first chapter (Introduction), the thesis subject is presented as well as a background and objectives of the project.

In the second chapter (Literature review), it is made an introduction to adhesives, described how thermal chambers are usually done, and presented some commercial examples of *Tg* machines, torsion machines, and thermal chambers.

In the third chapter (Thermal chamber design), all the stages towards the final design are described and analyzed. For such, all the materials and dimensions are defined and thermal simulations are performed to validate the thermal chamber design.

In the fourth chapter (Automation project), principles of temperature control are analyzed and the project of all the electronic/electric components of the system is explained.

In the fifth chapter (Conclusions), the main points of the thesis are summarized and the fundamental conclusions of the work are presented. There are also provided some suggestions for further improvements.

2 Literature review

2.1 Introduction to adhesives

Adhesives are materials that have the ability to hold parts in contact through a bond between their surfaces. There are two types of adhesives, the structural adhesives, and the non-structural adhesives. The structural adhesives are used as a connection capable of transferring structural loads, without the structural integrity of the bond being lost (Kosmač, 2013).

As such, structural adhesives are materials that have been more and more used in engineering projects, making necessary the study and knowledge of their properties. It is important to notice that the adhesives mechanical properties are deeply dependent on temperature and on their deformation history (Zhang *et al*, 2013).

Then, an important property of adhesives is the glass transition temperature, *Tg*, that corresponds to the temperature at which the liquid to glass, or rubber to glass, state transition occurs. The knowledge of this temperature is very important because it normally is close to the operating temperature of the adhesive. Bellow this temperature the adhesive has a glassy behavior (restricted movement of its atoms) and above it presents a behavior similar to a rubber (free movement of its atoms), thus losing the ability to behave as a structural bond (Hutchinson, 2009).

The stress-strain behavior of materials provides valuable information of the applicability of materials to certain engineering applications. In adhesive joints, there are several types of loads, being those that generate shear stress the most interesting to evaluate, since the joints are usually more resistant when this type of stress is applied. This is because all bonded area contributes to counteract the applied loads (da Silva *et al*, 2007).

2.2 Thermal analysis and methods to determine *Tg*

Thermal analysis (TA) is the study of the relation between a property of a sample and its temperature. This study is done with the sample being heated or cooled in a controlled way (Lever *et al*, 2014).

The thermal analysis is constituted of several methods nevertheless, not all of them are capable of determining what the glass transition temperature of an adhesive is. So, according to literature, the methods that have currently been used with greater reliability for the determination of the *Tg* are (Hutchinson, 2009, Zhang et al, 2013):

- *Thermomechanical analysis* (TMA);
- *Dynamic mechanical thermal analysis* (DMTA);
- *Differential scanning calorimetry* (DSC).

The *Tg* machine of the ADFEUP laboratory is based on the DMTA method and so a brief description of the method will be presented below.

2.2.1 *Dynamic mechanical thermal analysis* (DMTA)

DMTA is the most popular thermal analysis method to characterize viscoelastic properties of a material since it can be easily adapted for studies of both solid and liquid polymeric materials.

In most of the commercial machines, this method involves imposing a small cyclic strain on the sample and then measuring the resulting stress and strain response. The test is done in a controllable thermal chamber. The sample can be tested in a temperature range that can go from -150 to 500 °C with a heating/cooling rate from 0.1 to 5 °C/min (Menczel and Prime, 2014).

Some of the applications of this method are (Menczel and Prime, 2014):

- Determination of mechanical properties such as the damping of viscoelastic materials, over a temperature and time (frequency) domain;
- Determination of the glass transition temperature;
- Determination of the curing of networks.

For the determination of the glass transition temperature through the DMTA, it is necessary to evaluate the response of either the storage modulus, E', the loss modulus, E'', and the loss tangent (loss factor), tanδ. The storage modulus represents the elastic recoverable energy during deformation, the loss modulus represents the energy lost in the form of heat as a result of the interaction of the molecular chains while deformation occurs, and the loss tangent is the ratio between the loss modulus and the storage modulus. Typical curves of these properties as a function of temperature are represented in the graph of Figure 2.1.

There are three principles to determine the *Tg* (Li *et al*, 2000):

1. Intersection of the storage modulus curve with the loss modulus curve;
2. Higher value of the loss modulus curve;

3. Higher value of the loss tangent.

As we can see in the graph of Figure 2.1, the glass transition temperature is not the same for each principle, so it is necessary to choose one of these criteria to determine the *Tg*. Li et al (2000) verified that the principle that obtains better results for the *Tg* is the principle of the higher value of the loss modulus.

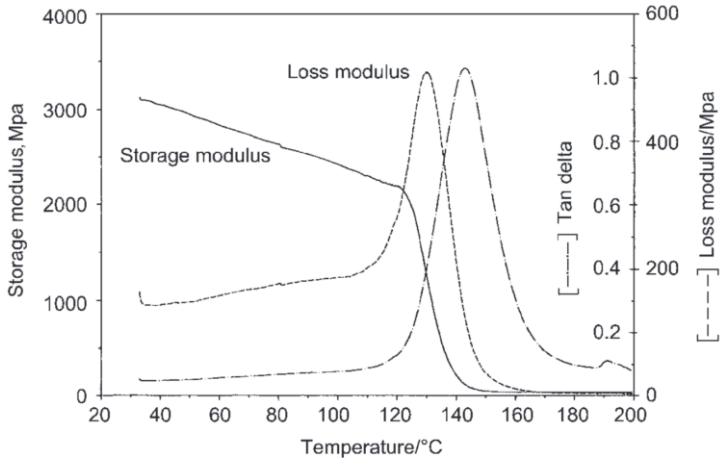

Figure 2.1 - Representation of the storage modulus, loss modulus and loss tangent (in the graph "tan delta") for an epoxy in function of temperature (Li et al, 2000).

2.3 Existing *Tg* machine and operation principle

The machine that determines the glass transition temperature existent in the ADFEUP laboratory was done in several previous dissertations. This machine is based on the DMTA method, but instead of using a small cyclic strain, the specimen is placed to vibrate at the resonance frequency. The configuration of the specimen is represented in Figure 2.2. The vibration of the beam is accomplished by a magnet placed at one end of the beam. The magnet will be attracted or repulsed from a drive coil that will generate a variable magnetic force. The drive coil will be controlled, so that the specimen can vibrate at the resonance frequency. The controller knows if the beam is on resonance because at the other end of the beam is placed another magnet that when vibrating will induce an electric signal in the pickup coil. This signal will be passed to the controller to know how the beam is vibrating. The vibrating beam is held on two wires that are placed exactly at the nodes of the vibration so that they cannot interfere with the vibration mode of the specimen. During all the test, the amplitude of vibration of the specimen is measured, while the temperature is varying. We know that the damping is inverse to the amplitude of vibration, so the damping reaches a maximum value when the amplitude of vibration reaches a minimum value. The temperature on which the maximum value of response occurs is the glass transition temperature. To correctly measure the temperature a dummy beam

is utilized, placing a thermocouple in the sample of that beam. This is necessary because if we place the thermocouple in the vibrating beam, the vibration mode will change.

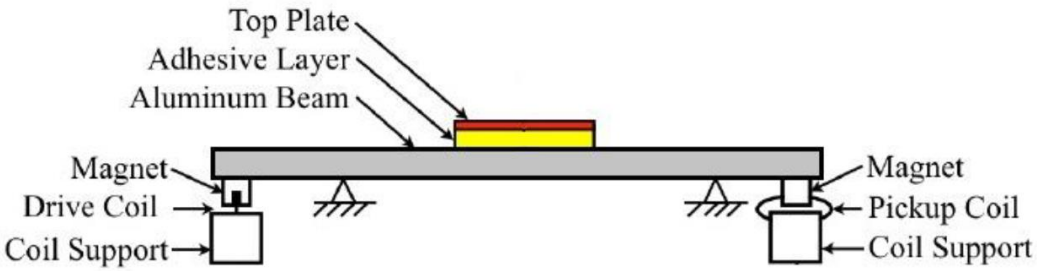

Figure 2.2 - Configuration of the vibrating beam (Daniel, 2013).

2.4 Methods to determine shear properties

To determine the shear properties of an adhesive two types of shear tests can be made, the bulk and the joint tests. The joint tests are more accurate, nevertheless sometimes the displacement is so small that it is difficult to measure. The bulk specimen tests are easily measurable, but the properties obtained are not representative of the adhesive behavior in a joint (da Silva *et al*, 2011).

The tests that can be done to determine adhesive shear properties are (da Silva et al, 2011):

1. Bulk specimens:
    a. Bulk torsion;
    b. V-notched beam shear method (Iosipescu);
    c. Notched plate shear method (Arcan).
2. Joint specimens:
    a. Arcan joint method;
    b. Iosipescu joint method;
    c. Butt joint in torsion;
    d. Thick adherend shear test (TAST);
    e. Single lap joint (SLJ);
    f. Pin-and-Collar Test.

From these methods, the ones that give better results are the methods that apply torsional moments. This is because no bending stress, or other types of stress besides shear stress occur. So, in these methods, we obtain clean shear properties. But these methods are little used, because the machines and measuring equipment required are complex and so, less available (da Silva et al, 2007).

The methods implemented in torsion machines are the bulk torsion and the butt joint in torsion.

The bulk torsion is basically a solid or tubular bar of adhesive that is placed in rotation. There is no normalization for the dimensions of the specimens, varying from author to author (da Silva et al, 2011).

In the butt joint in torsion, the specimen is constituted of two bonded substrates, that can be solid or tubular. In Figure 2.3 and Figure 2.4 are represented the two alternative geometries (da Silva et al, 2011).

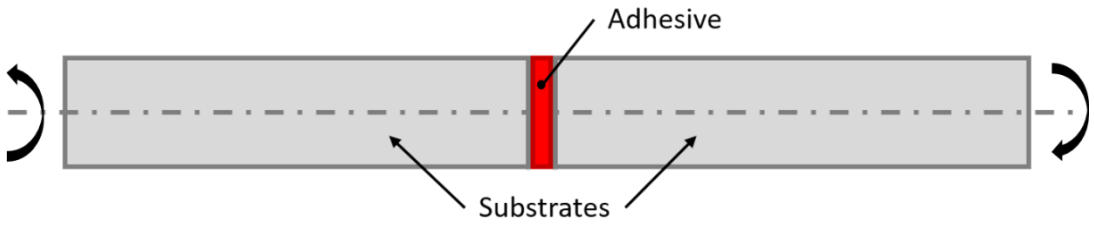

Figure 2.3 - Butt joint in torsion with solid adherends.

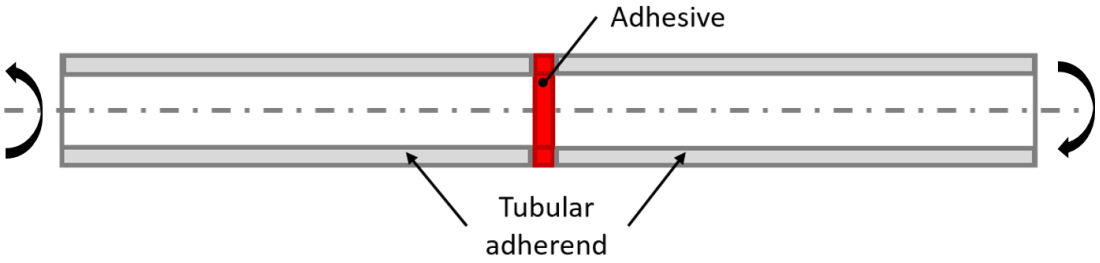

Figure 2.4 - Butt joint in torsion with tube adherends.

2.5 Existing torsion machine

Because the best way to determinate the shear properties of an adhesive joint is by applying a torsional moment, in the ADFEUP laboratory we have a torsion machine to test adhesives. This machine was developed previously in several theses and will be briefly presented below.

As we can see in Figure 2.5, the torsion machine is composed of several components and it is positioned in the vertical direction. The machine includes two chucks that will grab the specimen. Both chucks are connected to a set of self-aligning ball bearing and torsionally rigid coupling. These components have the objective of absorbing loads that are not torsional. This is required when the specimen in not perfectly aligned.

The bottom chuck, self-aligning ball bearing, and torsionally rigid coupling are connected to a servomotor with a reducer. The upper chuck, self-aligning ball bearing and torsionally rigid coupling are connected to a torque cell to measure the torque that is being applied by the

servomotor. All these top components are fixed to a moving cart that will translate vertically along linear guides to accommodate different length specimens. To prevent these components from falling, a counterweight is utilized.

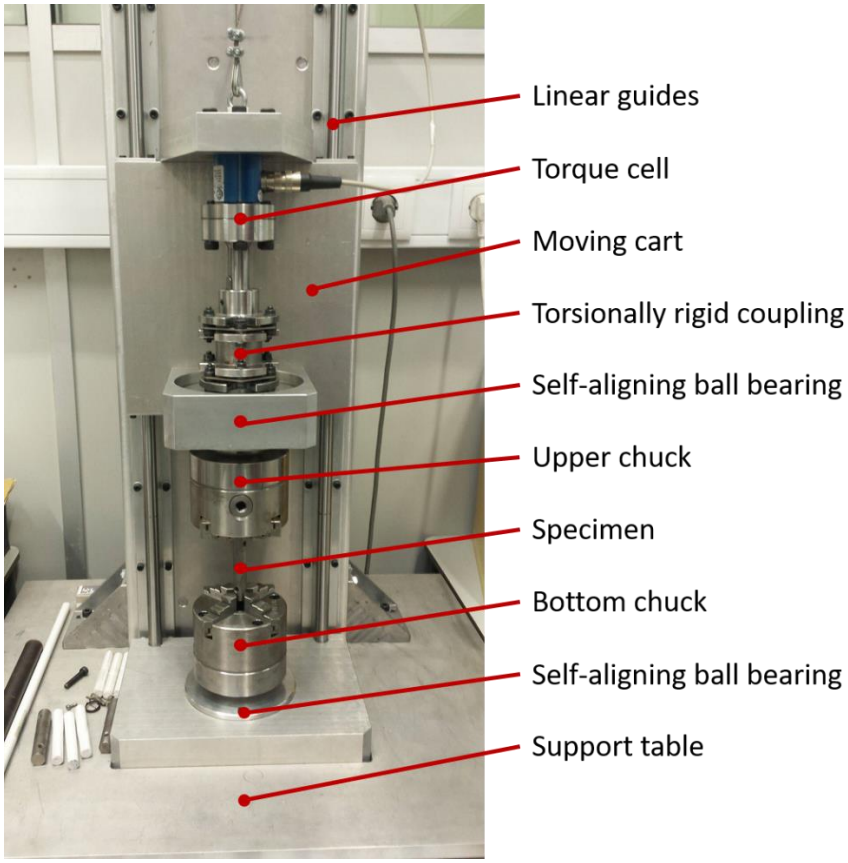

Figure 2.5 - The front perspective of the torsion machine existent at adhesives laboratory.

The bottom torsionally rigid coupling, the reducer, and the servomotor are located under the support table and the counterweight is in the back of the structure.

2.6 State of the art of thermal chambers

Before the design of the thermal chamber, a literature review of thermal chambers that are utilized for testing materials was done, in order to have a starting point to the design of the thermal chamber.

From the literature review, it is possible to deduce that thermal chamber walls are always constituted of a sandwich structure, Figure 2.6. This sandwich structure usually comprises three layers, being the interior and the exterior made of a structural material, normally stainless steel or aluminum. The intermediate layer is made of an insulation material. From the literature, the insulation material varies a lot from author to author, being a material such as rock wool, glass wool, rigid ceramic or cork (SIGMA, 2000, Gunnarsen *et al*, 1994, Zarr *et al*, 1995).

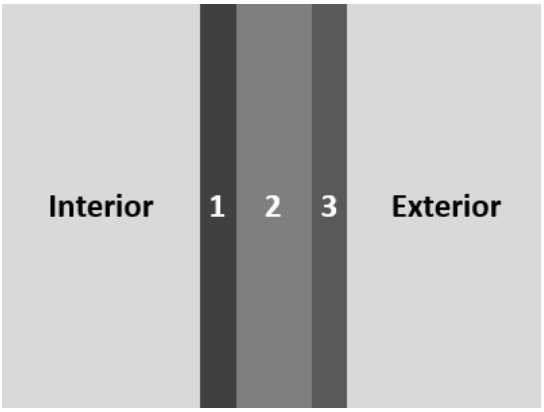

Figure 2.6 - Representation of the sandwich structure of a thermal chamber. 1 - interior layer; 2 - insulation material; 3 - exterior layer.

When building the structure of the thermal chamber we need to take care of the insulation material. This material needs to be completely covered because the ambient air has some humidity and when heating, this humidity will tend to condense. If the insulation material is not completely covered, this condensed humidity will soak and ultimately saturate the insulation material, which would lead to the loss of its insulation capabilities.

There are several types of connections to make the joints of the wall of the chamber. These joints are mostly welded, riveted or screwed. The welded joints are the most effective and advisable type of connection, but this method, as the riveted one, leads to permanent connections. The screwed method is not permanent, but can have some problems if vibrations are involved. In the end, the three methods are possible to be utilized, and it is a matter of choice and applicability.

Because the thermal chamber is required to operate at the range of temperatures of -100 to 200 °C, a description of heating and cooling systems is presented.

2.6.1 Heating system

The heating process can be done by natural convection. The air heated at the inferior zone of the chamber will move upwards in the interior of the chamber. This method has the problem of resulting in a non-homogeneous temperature along the vertical direction.

There is also a method that is based on forced convection. For this, a fan creates an airflow that will pass through a heating element. The heated air is mixed in the thermal chamber. This can be done with a heating element in a secondary chamber that heats the air and a fan that sends the air to the main chamber. Alternatively, the heating element can be in the main chamber and the air flow created there will make the air cross through the heating element (Portugal, 2004).

The heating element is normally done by the electric current going through a resistive element. This resistive element, by Joule's law, will dissipate energy through the form of heat. Is that heat that will increase the temperature inside the chamber. There are several types of heating elements, varying in shape, dimension, and material. Normally the heating elements are divided into three groups, Figure 2.7 (Group, 2017):

- Molybdenum disilicide ($MoSi_2$) heating element;
- Silicon carbide (SiC) heating element;
- Metallic heating element.

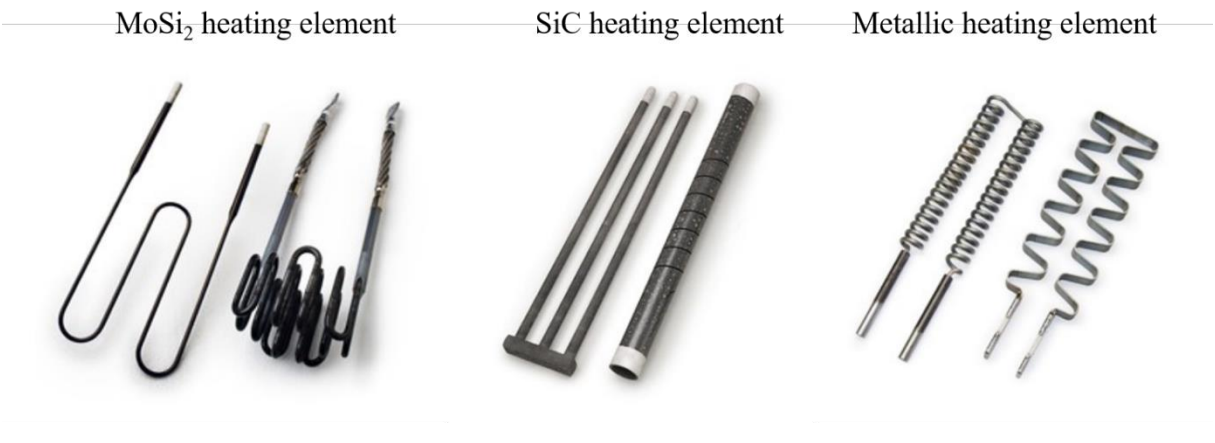

Figure 2.7 - Groups of heating elements from KANTHAL (Group, 2017).

The metallic heating elements are made from wire or strip. So, if we want a shape or dimensions that are not available, we can buy a resistive material in wire or strip and make our own heating element. These types of metallic wires or strips can be made of (Group, 2017):

- High resistivity iron-chromium-aluminium alloy (FeCrAl);
- High resistivity nickel-chromium alloy (NiCr);
- Low resistivity nickel-iron alloy (NiFe);
- Medium and low resistivity copper-nickel alloy (CuNi).

Another type of heating elements is a spiral/coil heating resistance made of wire, for example from nickel-chrome, Figure 2.8.

Figure 2.8 - Spiral/Coil heating elements (Inc., 2017).

2.6.2 Cooling system

There are two main types of cooling mechanisms. One is mechanical cooling and the other is cryogenic cooling. The mechanical cooling is well known and easy to use but limited because it does not allow to cool to temperatures as low as cryogenic cooling. Although cryogenic cooling allows getting lower temperatures, it is required to take some precautions when using a cryogenic coolant like nitrogen or carbon dioxide. These cryogenic gases are not toxic and are present in atmosphere, but if the cryogenic gas usage is high, or the laboratory where the test is done is small and has a low air volume and poor ventilation, then there is a chance that the breathable oxygen present in the air is dissipated, and so the oxygen levels in the air will be lower than the recommended (SIGMA, 2000).

In Figure 2.9 is represented a typical mechanical cooling system and a typical cryogenic cooling system. The mechanical one is a closed system and so it is necessary a condenser and an evaporator for the heat transfer between the fluid and the exterior. From the condenser to the evaporator it is required a compressor and between the evaporator and the condenser, it is required a throttling device and a metering valve. The cryogenic system just needs the coolant source, the metering valve, a fail-safe valve and the throttling device. The mechanical system is easy to use since it is self-contained, but it is limited because it is dependent on the compressor capacity, that is dependent on the available space, power, and tolerance to heat and noise. The cryogenic system is much less limited because nitrogen has an evaporation temperature of -195.8 °C. Another advantage of cryogenic systems is the fact that the coolant is already bought compressed and so are required much fewer components, and so the installation is more compact and cheaper. But, the coolant source is expensive and if it is not required to reach a low temperature, or if it is not required to have a fast cooling rate, then for applications of few

uses, the cryogenic system will be more expensive, because the cheaper installation will not compensate the expensive coolant source (SIGMA, 2000).

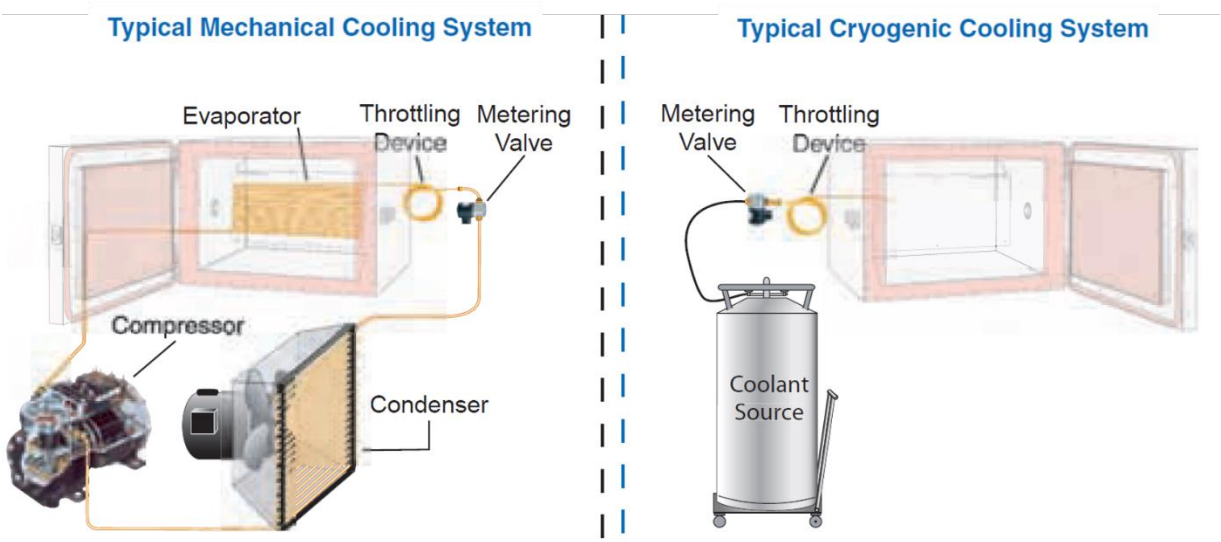

Figure 2.9 - A typical mechanical cooling system on the left and a typical cryogenic cooling system on the right (SIGMA, 2000).

2.6.3 Commercial thermal chambers

TA Instruments is a U.S. company specialized in the production of equipment for thermal analysis tests, such as DSC and DMTA method. This company has thermal chambers that are capable of testing samples in a temperature range of -150 to 350 °C, Figure 2.10. This chamber is connected to a computer to perform the tests at a constant or variable temperature. The heating process is done internally by electric resistances and the cooling process is done externally (Instruments, 2016).

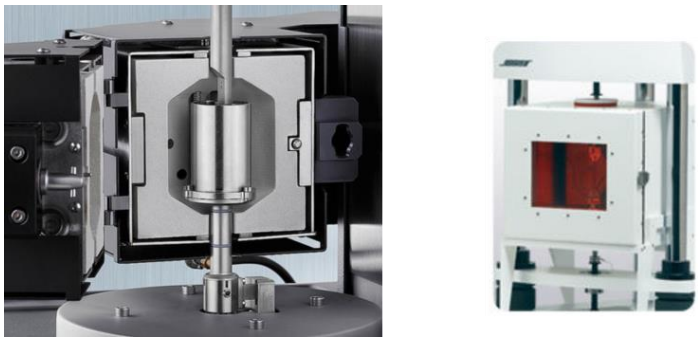

Figure 2.10 - TA Instruments hot/cold chamber (Instruments, 2016).

For the cooling process, TA Instruments has mechanical and cryogenic cooling solutions. The mechanical solution (RCS90), is capable of cooling the interior of the thermal chamber to temperatures of -90 °C, and only needs to be connected to the electric power supply, so it is more power efficient than the cryogenic solution. This mechanism has several temperature

cooling velocities, but when we want to go to temperatures close to the -90 °C the cooling velocity is slow (Dallas and Aubuchon, 2016).

Figure 2.11 RCS90 refrigeration system (Dallas and Aubuchon, 2016).

The cryogenic cooling system is based on nitrogen (LNCS), and because of that the lower operating temperature can be -180 °C and has a cooling velocity that can go to 140 °C/min. In Figure 2.12 is represented the LNCS cooling system that is refrigerating the chamber of a DSC Q2000 (Dallas and Aubuchon, 2016).

Figure 2.12 - LNCS cooling system refrigerating the chamber of a DSC Q2000 (Dallas and Aubuchon, 2016).

3 Thermal chamber design

In this chapter, are presented the structure and the dimensions of the thermal chamber so that it can be used both in the glass transition temperature machine and the torsion machine. A continuous and parallel work was made, involving thermal and flow simulation in SolidWorks, to validate the thermal chamber design and dimensions. These simulations, consider the principles of heat and mass transfer. As so, this chapter will begin with some concepts and principles of heat transfer.

3.1 Heat transfer concepts and principles

Heat transfer means energy in the form of heat that travels from one place to another due to a spatial temperature difference. There are three main types of heat transfer, Figure 3.1:

- Conduction;
- Convection;
- Radiation.

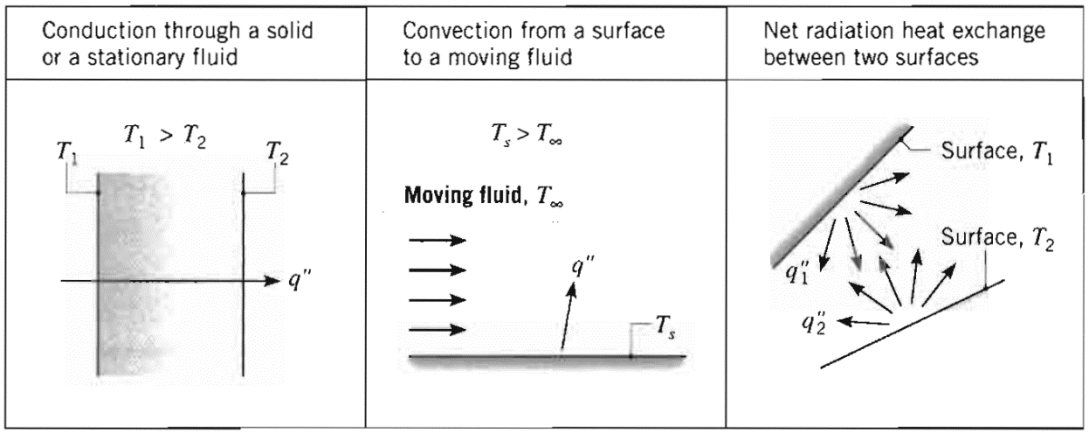

Figure 3.1 - Scheme of the three types of heat transfer (Bergman and Incropera, 2011).

Conduction corresponds to the transfer of energy from particles with more energy to particles with less energy of a substance. This heat transfer is due to the interaction between particles. To determine and quantify heat transfer in conduction, we utilize the Fourier's law that gives us the energy that is being transferred per unit of time. For a one-dimensional space, the Fourier's law is presented in Equation 3.1 (Bergman and Incropera, 2011):

$$q''_x = -k \cdot \frac{dT}{dx}, \quad (3.1)$$

where the variables are:

q''_x - heat flux, or amount of energy transferred per unit of time, measured in W/m^2;

T(x) - temperature distribution;

k - thermal conductivity, measured in W/(m·K).

Convection is the transfer of heat by the actual movement of warmed/cooled matter. Convection includes two mechanisms: diffusion, that is the heat transfer due to random molecular motion, and heat transfer, due to a macroscopic motion of the fluid. The equation that evaluates the quantity of energy transferred from convection is known as Newton's law of cooling and is represented by Equation 3.2 (Bergman and Incropera, 2011):

$$q'' = h(T_s - T_\infty), \quad (3.2)$$

where:

q'' - convective heat flux, measured in W/m^2;

T_s - temperature of the surface in °C;

T_∞ - temperature of the fluid in °C;

h - convection heat transfer coefficient, measured in W/(m^2·K).

Convection can be divided in forced convection and natural convection. In forced convection, the movement of the fluid is externally imposed, while in natural convection the movement of the fluid is due to buoyancy forces within the fluid (Bergman and Incropera, 2011).

Radiation is the energy emitted trough electromagnetic waves by all the substances that have a temperature greater than 0 K. The heat transfer in radiation does not require a material medium. To quantify the energy that is emitted from a surface per unit area by radiation, we utilize the Stefan-Boltzmann law that is represented by Equation 3.3 (Bergman and Incropera, 2011):

$$E = \varepsilon \cdot \sigma \cdot T_s^4, \quad (3.3)$$

where:

E - heat power emitted by a real surface in W/m^2;

ε - radiative property of a surface known as emissivity, that can take values from 0 to 1;

σ - Stefan-Boltzmann constant (5.67x10^{-8} W/(m^2·K));

T_s - temperature of the surface in K;

3.2 Thermal chamber materials

As mentioned before, the thermal chambers are normally made of a sandwich structure composed of three layers. In our case, the materials selected are stainless steel, for the internal and external layer, and rock wool, for the middle insulation layer. The stainless steel was selected since it is a cheap structural material and because it has a substantially lower thermal conductivity than aluminum, Table 3.1. For the insulation layer, the chosen material was rock wool, since it is a material with a very low thermal conductivity, it is cheap and has an operating temperature between -200 and 800°C. The rock wool can be purchased in FIBROSOM company and some of the material properties are indicated in Table 3.2.

Table 3.1 - Thermal conductivity of aluminum and stainless steel.

	Thermal conductivity at 20°C ($W \cdot m^{-1} \cdot K^{-1}$)
Aluminum	200
Stainless steel	17
Rock wool	0.034

Table 3.2 - Properties of FIBROSOM rock wool material (Fibrosom, 2017).

Thermal conductivity ($W \cdot m^{-1} \cdot K^{-1}$)	0.034
Thickness (mm)	30 - 60
Fire classification	A1
Thermal resistance ($m^2 \cdot K/W$)	0.85 - 1.75

3.3 Thermal chamber dimensional limitations

Since the thermal chamber will be used for testing adhesives in two different machines, some care is needed when choosing its shape, so that it can comply with the requirements of space and shape of both testing machines. As such, we need to analyze the free space on each machine.

In the case of the glass transition temperature machine, there are two specimens placed horizontally, as represented in Figure 3.2. Considering that neither the coils nor the electronic components can be inside the chamber, the maximum exterior length along the samples will be 110 mm, and the maximum distance between the bottom of the chamber and the samples will be 125mm.

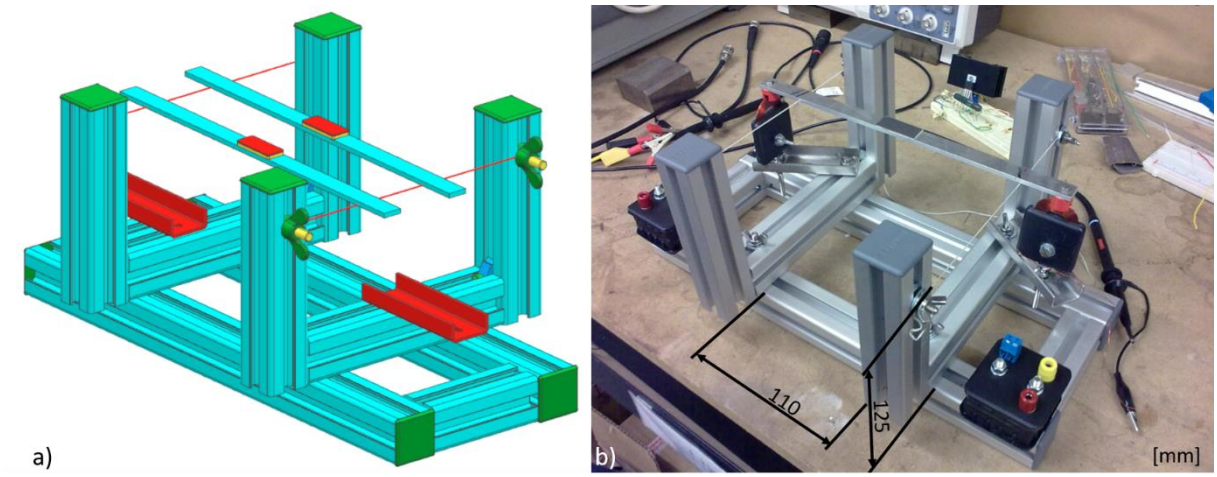

Figure 3.2 - a) 3D drawing of the structure of the Tg machine with both samples; b) Structure of the Tg machine mounted with Minitec components, only with the sample subjected to vibration. (Telha, 2012).

In the case of the torsion machine, the specimen is along the vertical axis, Figure 3.3, and the thermal chamber cannot cover the chucks since it was recommended by the manufacturer that the lathe chucks should not be subjected to temperatures over 40 ºC due to the lubricant used. So, for this machine, when thinking about the solution for the thermal chamber, we need to consider that the length through the vertical axis needs to be between 75 and 150 mm, because the samples used need to have dimensions into this interval. In this machine, we also consider the depth of the chamber, since the distance between the center of the chucks and the guides of the mobile structure is 85 mm, as seen in Figure 3.3.

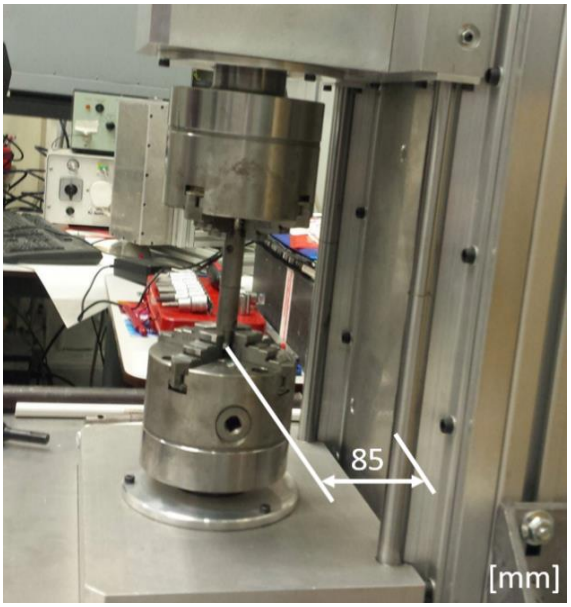

Figure 3.3 - The lateral perspective of the torsion machine at the chucks zone, with the sample mounted.

Taking into account all dimensional limitations and considering that it is required that the chamber has an opening plane, to be easier to place the specimens into position, and to be simpler the process of changing specimens over several tests, it was thought to make a thermal

chamber with cylindrical shape, consisting of two halves. One of the halves will be fixed and the other one will move in relation to the first one, to allow the opening of the chamber. This concept is represented in Figure 3.4, considering that the thermal chamber will be along the horizontal axis, in the case of the Tg machine, and along the vertical axis, in the torsion machine.

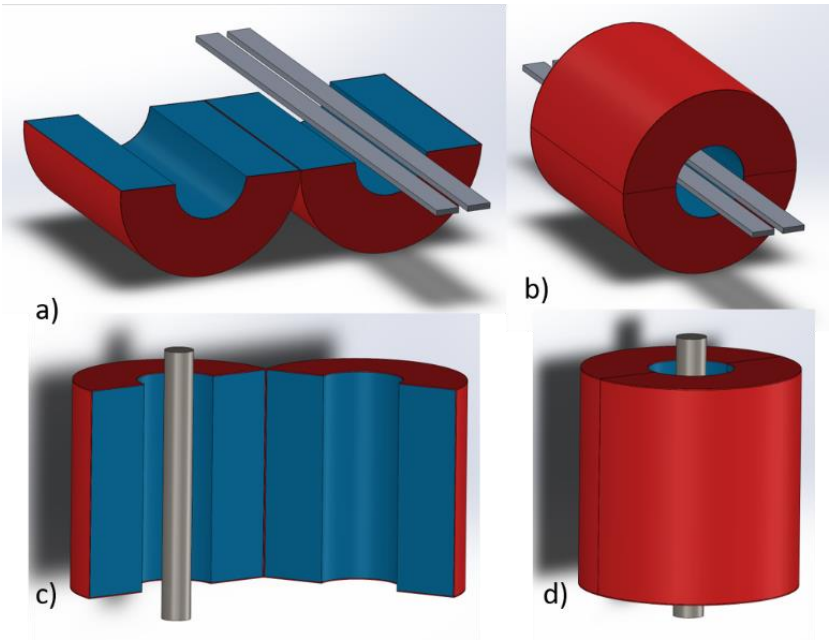

Figure 3.4 - a) e b) Thermal chamber placed on the Tg machine through horizontal, opened and closed, respectively; c) e d) Thermal chamber placed on the torsion machine through vertical opened and closed, respectively.

After this analysis, it is known that the maximum height of the cylinder chamber may be 110 mm and the maximum radius 85 mm. In terms of the interior dimensions of the cylinder, we need to know the specimens shapes and dimensions, and also consider that the heating element will be inside the thermal chamber.

In the case of the torsion machine, the specimen has a cylindrical shape with a diameter of 14 mm. In the Tg machine, two specimens are needed. One specimen is vibrating and the other one is stationary, and serves to measure the evolution of the adhesive temperature. Both the specimens are equal, with section dimensions of 12.5x3 mm. Therefore, the critical dimensions are imposed by the Tg machine. Considering that the vibrating specimen needs to have some space to prevent accidental contact, preventing to interfere in the vibration mode, the recommended minimum interior diameter of the chamber will be 50 mm, Figure 3.5.

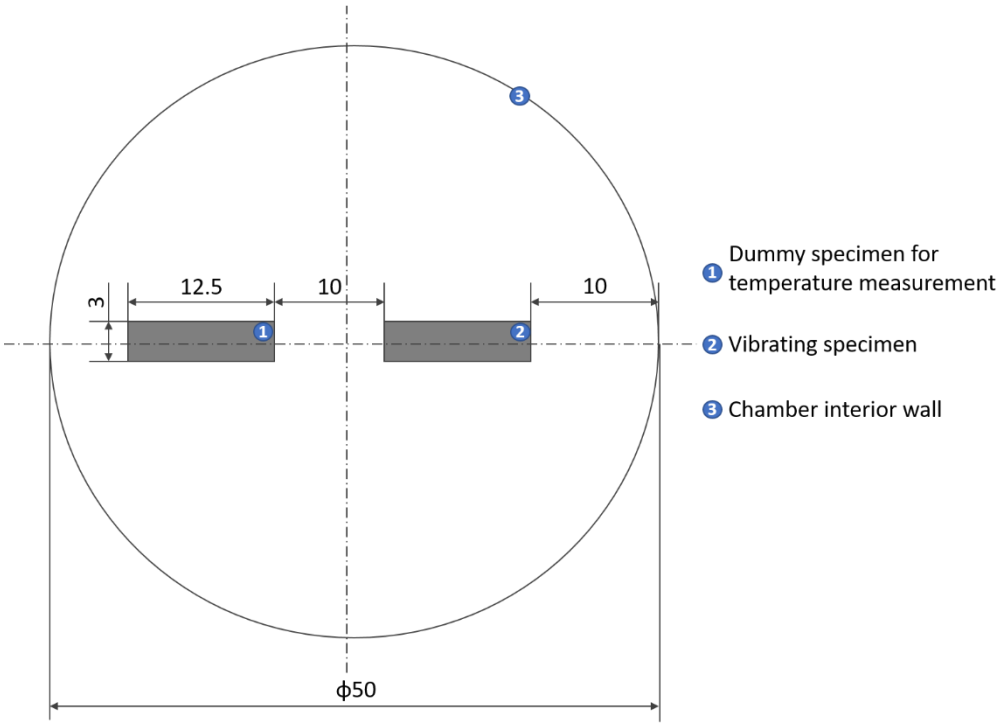

Figure 3.5 - Diagram of the recommended minimum interior diameter of the chamber.

However, these dimensions do not consider the space required for implementing the heating element in the interior of the chamber. To know the real interior dimensions, it is necessary to search for distinct types of heating elements, choosing the one that complies with the space and heating power required. Because the chamber is constituted of two halves, the heating system will comprise two heating elements, one in each half. The required power is 400 W. Therefore, we will use two heating elements of 200 W. A spiral resistance meets both dimensional and power requirements. This resistance is sold by *Saidacasca* and its characteristics are represented in Table 3.3.

Table 3.3 - Characteristics of the spiral resistance sold in *Saidacasca* (saidacasca, 2017).

Material	Nickel-chrome
Power	200 W
Supply voltage	220/230 VAC
Coil length	125 mm
Maximum coil length	1200 mm
Coil diameter	3 mm

With all considerations exposed, the thermal chamber will have an interior diameter of 60 mm and each spiral resistance will go through all the interior of the respective half chamber, as seen in Figure 3.6, so that the generated heat is uniform throughout the entire volume.

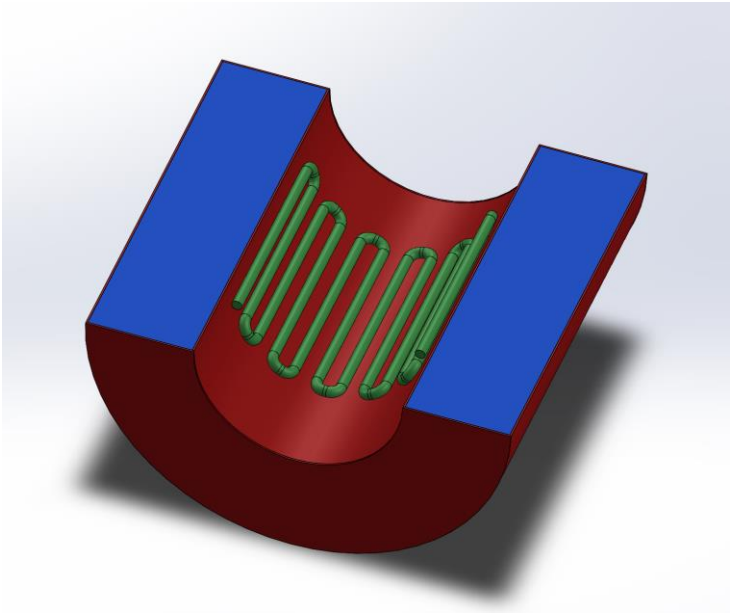

Figure 3.6 - Image of how the spiral resistance will be along the interior diameter of the chamber.

3.4 Methodology in SolidWorks flow simulation

To validate the design adopted for the thermal chamber, it is necessary to perform thermal and flow simulations. The simulations were done in the SolidWorks software, using the flow simulation add-in. Therefore, before explaining the experiments, a brief introduction to the software will follow.

The first step when doing a flow simulation is to define the type of analysis that is taking place, and what physical properties the software needs to consider, Figure 3.7. In the case of the thermal chamber, the analysis will be always an external flow, because the chamber is opened to the exterior. The properties that were selected in all simulations are the heat conduction in solids, the radiation, and gravity according to the vertical axis. Because the chamber is to be used in a laboratory, we considered in all simulations an environment temperature of 22 °C, and no solar radiation. According to what we want to obtain, we can choose a time-dependency or not. The time-dependency is important if we want to know the behavior of a model as a function of time, or if we want to know how long it takes to reach to a certain temperature. This type of analysis will be of great importance for the glass transition temperature machine. Before we define the boundary conditions of the simulations, it is important to specify the existing fluid, so that the software can consider the natural convection that such fluid will cause. In the case of the thermal chamber, the fluid is air.

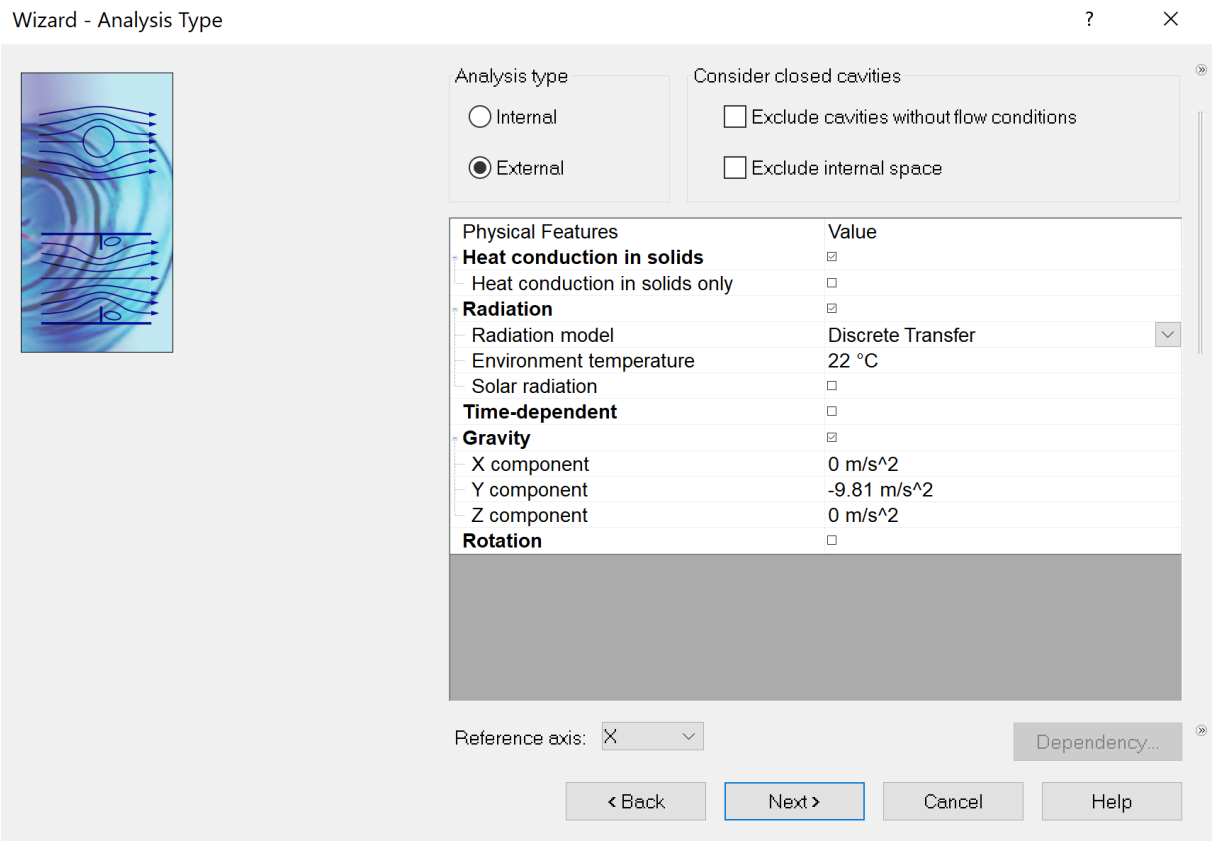

Figure 3.7 - Interface of the SolidWorks flow simulation wizard.

After defining these general properties related to the software, a new project is created and then it is required to define some more specific properties and boundary conditions.

So, we need to define the materials that are used in each element of the model. This can be done choosing materials from the software database. If some required materials do not exist in the SolidWorks database, then we can create new materials. This is necessary in order to assign the thermal conductivity of each part, so that the behavior of the material is correct during the simulation. This is also required to assign to each part its specific heat, in order to know how much energy, the material needs to increase a degree in its temperature. The thermal conductivity and specific heat of each material is represented in Table 3.4. The stainless steel and the rock wool are used in the chamber walls as referred before. The aluminum is used in the specimens of the Tg machine and the carbon steel is used in the specimen of the torsion machine. The adhesive used in the simulations is an epoxy.

Table 3.4 -Thermal conductivity and specific heat of the material used in the simulation.

	Thermal conductivity ($W \cdot m^{-1} \cdot K^{-1}$)	**Specific heat ($J \cdot kg^{-1} \cdot K^{-1}$)**
Stainless steel	17	530
Rock wool	0.034	840
Aluminum	200	900
Carbon steel	51.9	450
Adhesive (epoxy)	0.188	1000

Another important aspect to define is the radiant surfaces, that is all surfaces that are in contact with air and not with any other solid components. The software has a database with information about emissivity of each material, according to its surface quality.

Finally, it is necessary to define the boundary conditions depending on whether it is a heating or cooling process. If it is a heating process, it is necessary to define the power sources. In the case of the thermal chamber, the power sources are the resistances and we define the heat rate that they generate. If it is a cooling process, since it is done through injection of nitrogen, it is necessary to define the inlet volume flow and the temperature of the nitrogen.

The software automatically defines a volume of control and a mesh. If we want, we can change the volume of control. For the mesh, it is not possible to define the mesh dimensions, we can just define a level for the mesh that goes from 1 to 7, being the 7 the smallest mesh. The simulations were done with the values chosen automatically by the software, since a more refined mesh leads to a too long simulation time.

3.5 Chamber design and thermal simulations

The first design of the thermal chamber was based in the literature review, that is inspired in typical thermal chambers. This first design for the cylindrical thermal chamber consisted simply on two half cylinders, with a wall of two stainless steel sheets of 0.5 mm. Between these sheets a rock wool with a thickness of 30 mm was inserted. Because the chamber has a dimensional limitation along its axis, the insulation thickness on the top walls will be 19 mm. This configuration is represented in Figure 3.8.

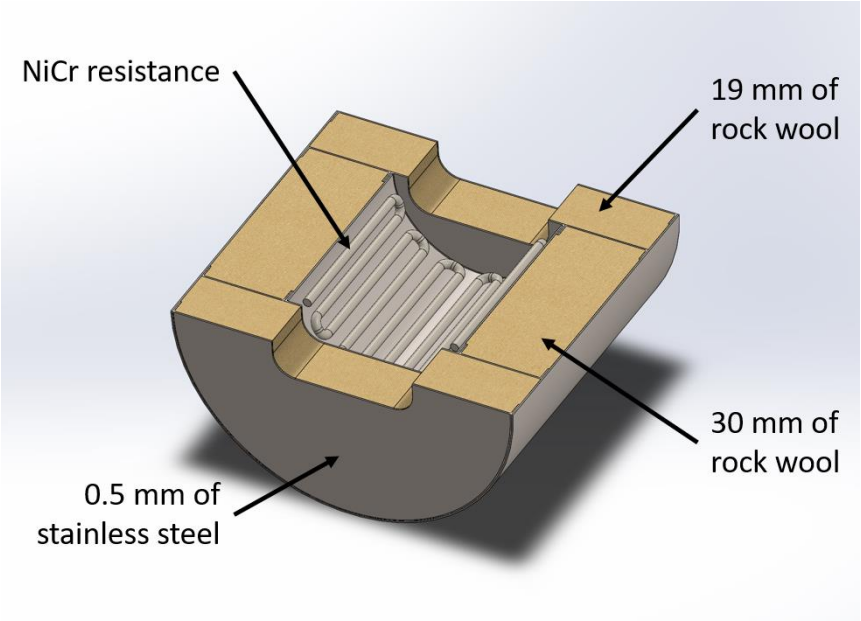

Figure 3.8 - One of the halves of the thermal chamber developed in the first model.

Two simulations were run to validate the design. One for the *Tg* machine and another for the torsion machine. In the flow simulations for this model, all materials and radiant surfaces were defined. The radiant surfaces are the exterior stainless steel surfaces, the interior stainless steel surfaces, the surface of the NiCr resistance and the surfaces of the adhesive (epoxy) exposed to air. For the Tg machine, the surfaces of the aluminum specimen are also included. For the torsion machine, the surfaces of the carbon steel specimen must be considered. Both simulations were performed for a heating process, and so it was necessary to define each resistance as a power source. No cooling simulation was done since in the heating simulation we verified that our design was inaccurate. In fact, we verified that the temperature in the exterior of the chamber was too high and could harm the user. The simulations results can be observed in Figure 3.9 and Figure 3.10.

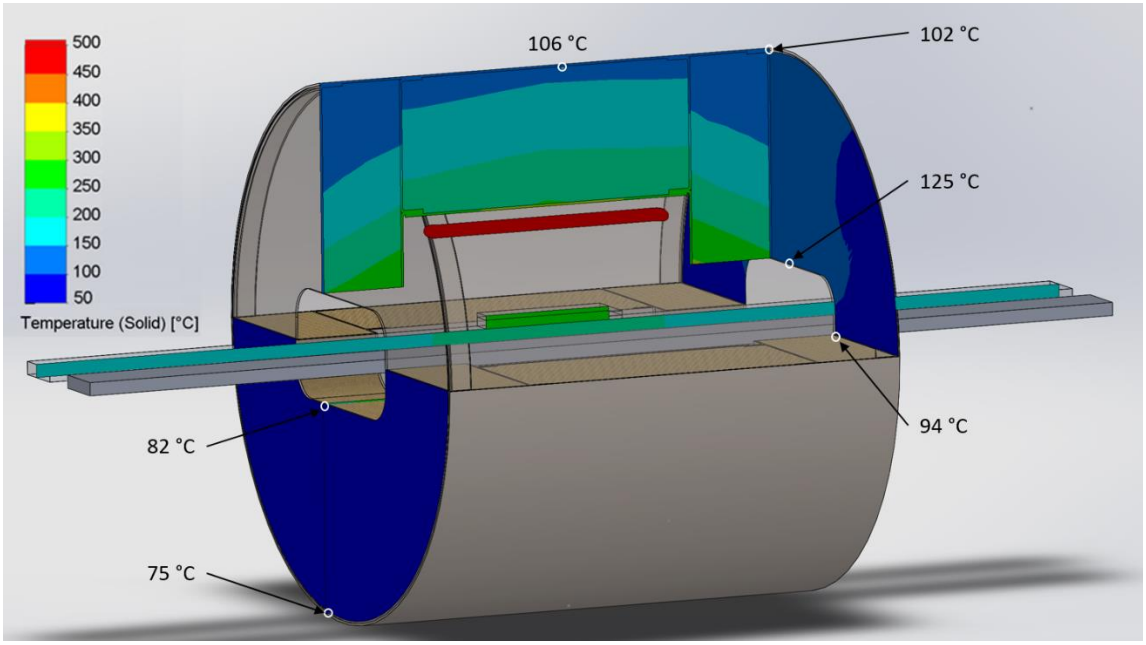

Figure 3.9 - Simulation in the *Tg* machine of the first design of the chamber for the heating process.

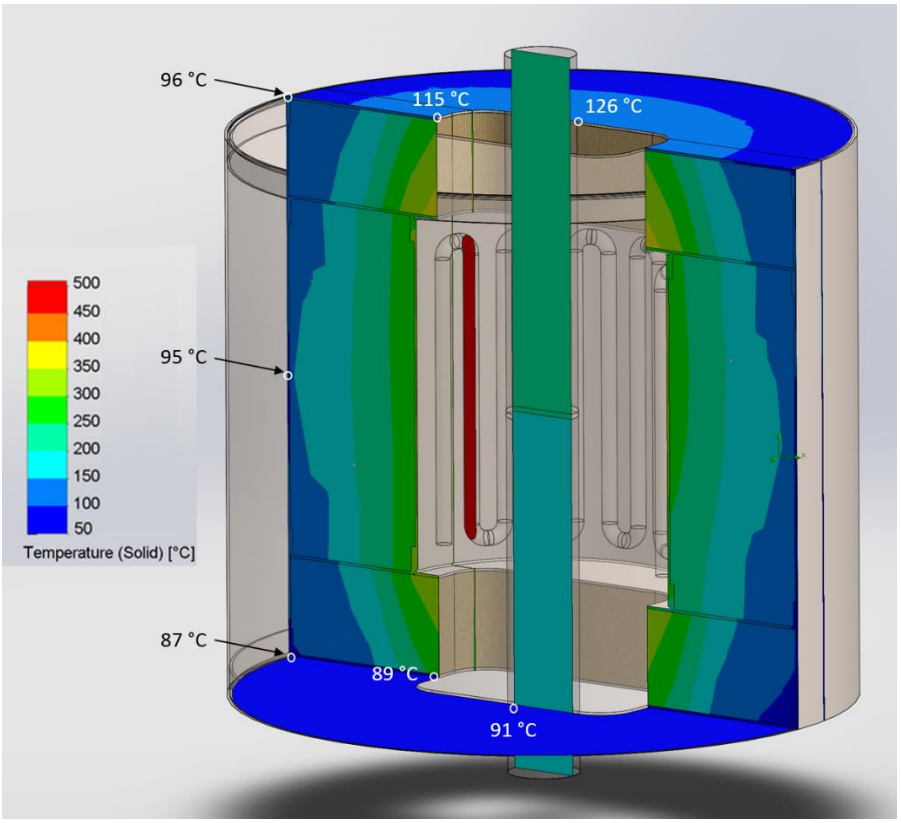

Figure 3.10 - Simulation in the torsion machine of the first design of the chamber for the heating process.

Because of the excessive temperature on the exterior surface of the chamber, a new design was proposed. This consisted of adding a new layer of air to the thermal chamber. Air is a good insulator, with a thermal conductivity of 0.027 $W \cdot kg^{-1} \cdot K^{-1}$. However, some care is needed because natural convection will occur if thickness is too large. The maximum thickness before natural convection starts is normally around 16 mm (Bergman and Incropera, 2011). If natural

convection exists, then the air layer will worsen the temperature behavior in the outer surface. So, the new design of the chamber will be similar to the previous one, but with an extra air layer with a 10 mm thickness. This design is represented in Figure 3.11.

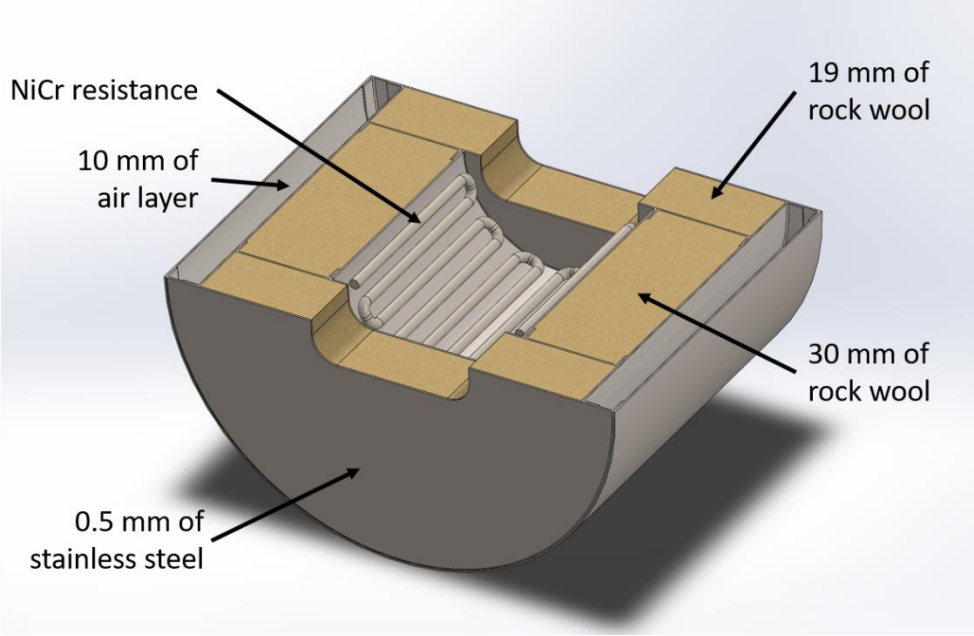

Figure 3.11 - One of the halves of the thermal chamber developed in the first model.

Two more simulations for the heating process were performed for this second design. The simulations were done assuming the same methodology and imposing the same boundary conditions of the first design. It was just necessary to define new radiant surfaces, which are the interior stainless steel on the air layer. The simulation results for this design are represented in Figure 3.12 and Figure 3.13.

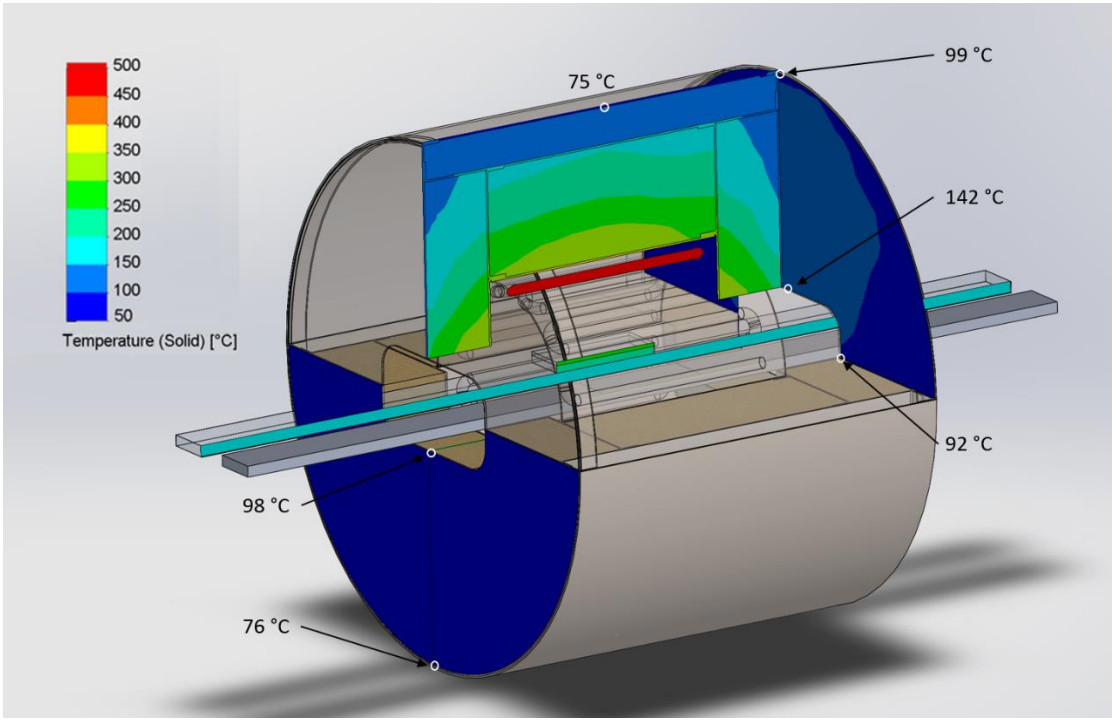

Figure 3.12 - Simulation in the *Tg* machine of the second design of the chamber for the heating process.

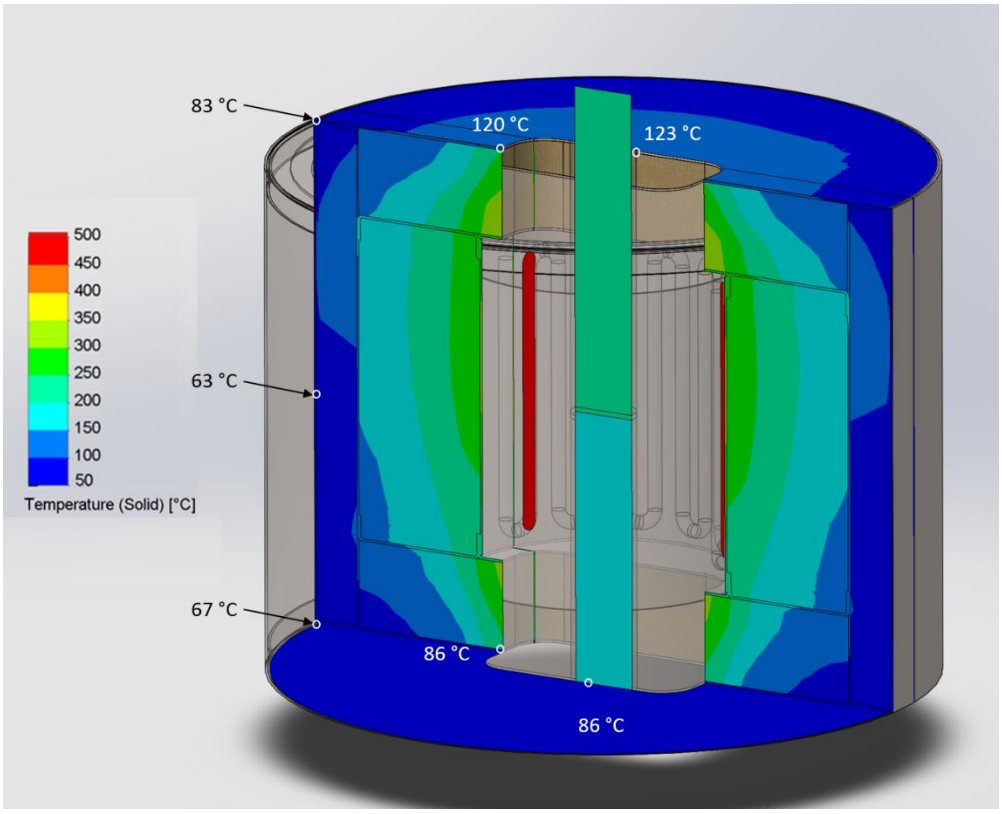

Figure 3.13 - Simulation in the torsion machine of the second design of the chamber for the heating process.

Analyzing the simulation results, we can see that the temperature in the lateral surface decreased compared to the first design. This was expected, nevertheless, the temperature is still too high, since the surface of the chamber should have temperatures closer to 50 °C to be safe for the

user. Another problem is the fact that we cannot add an exterior air layer at the tops of the chamber, which causes the temperature in the circular surfaces to be too high. In addition to the temperatures of the exterior surfaces, there is also a problem in homogenizing the temperature inside the chamber, mostly in the torsion machine. This problem is due to the natural convection of the air. The air, when heated, becomes less dense and therefore will go up. Because in the torsion machine the axis of the cylinder is in the vertical direction and the openings of the chamber are large, the air escape too fast. This will lead to a much higher temperature in the upper steel sample compared with the other one, which results into a higher temperature gradient in the torsion machine specimen. To lower the exterior surface temperatures to around 50 °C and to homogenize the temperature inside the thermal chamber, a new concept and design was idealized. This third design is represented in the Figure 3.14 for the *Tg* machine and in Figure 3.15 for the torsion machine.

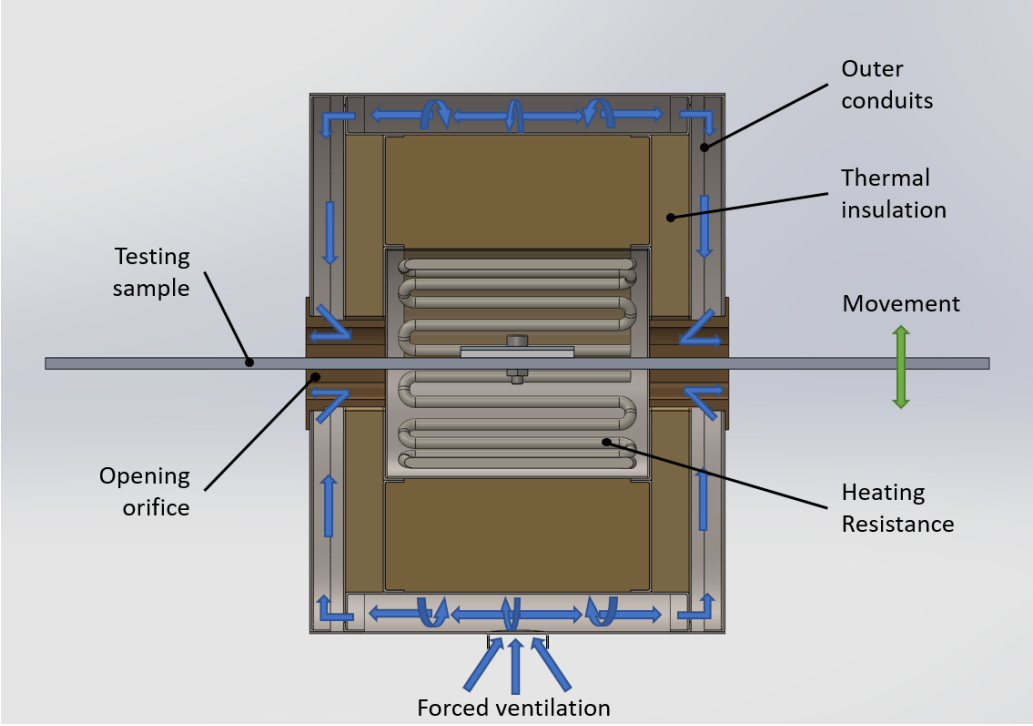

Figure 3.14 - Third design for the thermal chamber when used in the *Tg* machine.

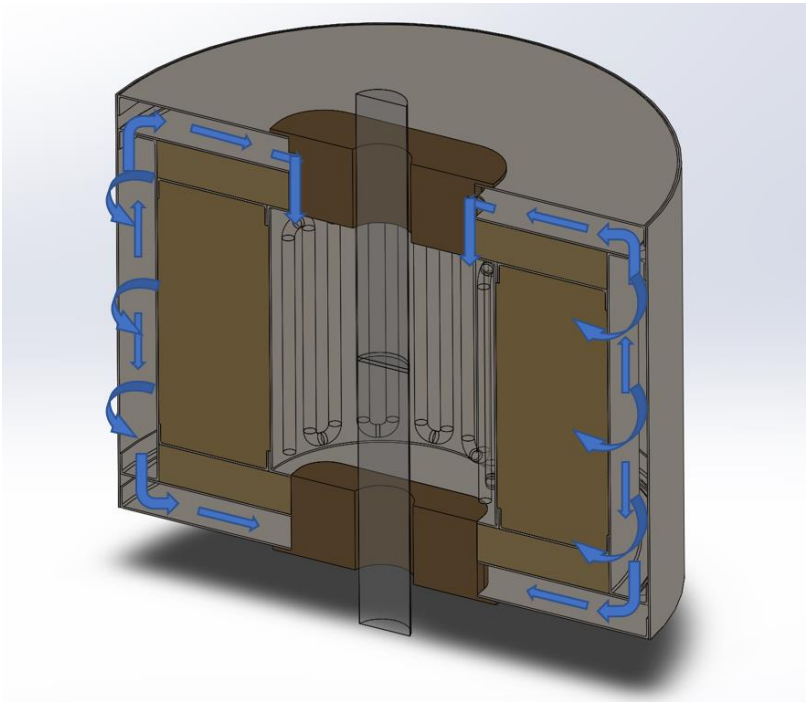

Figure 3.15 - Third design for the thermal chamber when used in the torsion machine.

As we can see, the new concept of the thermal chamber is based on the insertion of a forced airflow inside the insulation outer conduits of the chamber. These outer conduits are based on the outer air layer previously defined, and for the tops of the chamber, the insulation rock wool layer was shrunk to half the previous thickness, to have space for creating conduits also in these surfaces. The outer conduits of the tops are connected to the lateral conduit, which let the forced airflow to be redirected to the openings of the chamber (Figure 3.14 and Figure 3.15), in order to prevent excessive heat transfer between the interior and exterior of the chamber. This enables obtaining a homogenous temperature inside the chamber, as well as to avoid an excessive temperature gradient of the samples under test.

The forced air also enables the cooling/heating of the temperature of the outer wall of the chamber, so that the casing temperature does not reach extreme values.

The forced airflow is done using a fan that is placed as seen in the Figure 3.14, on the exterior of the fixed half of the chamber. This fan is constantly blowing air at the ambient temperature in the exterior conduits of the chamber. The chosen fan is from Sunon manufacturer and can be bought from the RS website. It is represented in the Figure 3.16 and its characteristics are represented in Table 3.5.

Figure 3.16 - Sunon DC axial fan utilized in the thermal chamber (RS, 2017a).

Table 3.5 - Characteristics of the Sunon DC fan utilized in the thermal chamber (RS, 2017a).

Supply voltage	5 VDC
Dimensions	17x17x8 mm
Air flow	1.5 m^3/h
Power consumption	0.8 W
Maximum current	160 mA
Fan speed	20,000 rpm

In the openings of the thermal chamber, cork covers are used for two reasons. First, to redirect the air flow in the openings as we want. Second, to prevent the overheat of the stainless steel top surfaces. This overheat occurs without the cork covers because the stainless steel has a considerably higher thermal conductivity and a lower specific heat than cork, Table 3.6, and when hot air escapes from the chamber, and contacts directly with the stainless steel surfaces, the temperature increases faster.

Table 3.6 - Thermal conductivity and specific heat of stainless steel and cork.

	Thermal conductivity ($W \cdot m^{-1} \cdot K^{-1}$)	**Specific heat ($J \cdot kg^{-1} \cdot K^{-1}$)**
Stainless steel	17	530
Cork	0.04	1700

It is important to notice that in the torsion machine the two cork covers are different. The bottom cover does not let pass the forced air flow. This is done because air has an ascending movement when it gets warmer. So, only the downwards air flow in the superior cork cover will exist to

counter natural movement of hot air, and then homogenize the temperature in the interior of the thermal chamber.

To do the simulations for the new design, the same criteria and boundary conditions used before were defined. It was just necessary to define a constant 1.5 m^3/h inlet volume flow of air at ambient temperature. Heating simulations for this design are represented in the Figure 3.17 and Figure 3.18. As we can see the temperature in the exterior surfaces is now acceptable to the human touch.

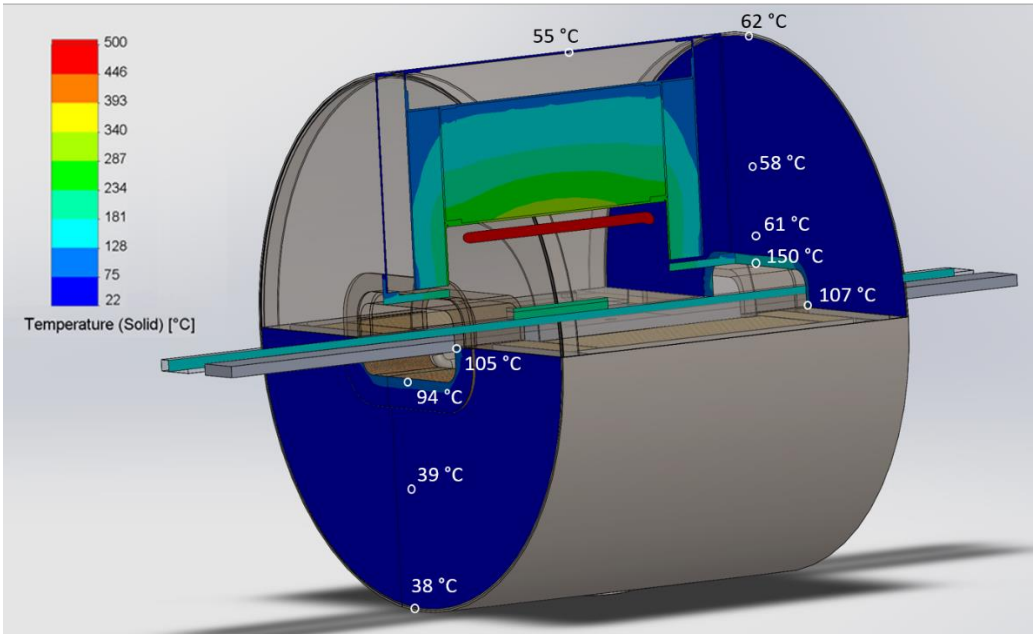

Figure 3.17 - Simulation in the *Tg* machine of the third design of the chamber for the heating process.

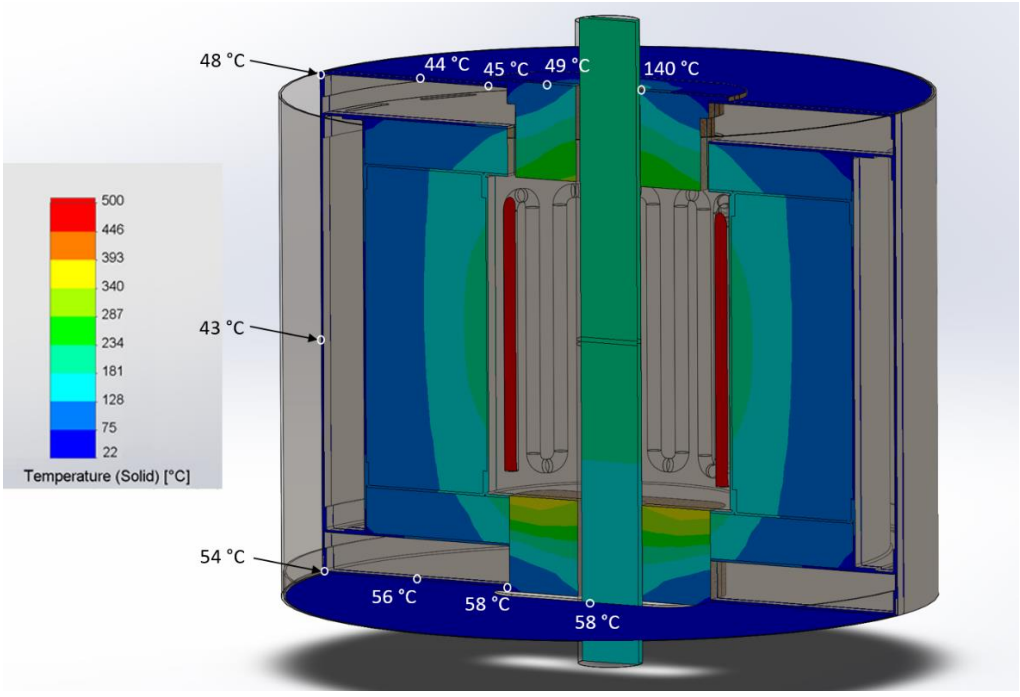

Figure 3.18 - Simulation in the torsion machine of the second design of the chamber for the heating process.

We can now conclude that, for the heating process, this third design is suitable for the thermal chamber. Nevertheless, it is also required to validate this design for cooling. In the exterior, the temperature of the surface should be higher than 3 °C for user protection.

To do the simulation of the cooling process, the same principles, and boundary conditions are applied. Because the cooling process will be done using a cryogenic solenoid valve, then it is just necessary to change the heating source for the injection of nitrogen. The injection of the nitrogen will go through a rigid pipe located in the fixed half chamber as seen in Figure 3.19. To define this boundary condition, we just define an inlet volume flow of nitrogen at the temperature of -180 °C. This temperature is justified because the nitrogen will decrease its temperature when passing from the tank to the chamber. The defined volume flow is 3.0 m^3/h, since the selected cryogenic solenoid valve is an Alcon 68 series with a pipe size of 3/8''. The properties of this valve are represented in Table 3.7.

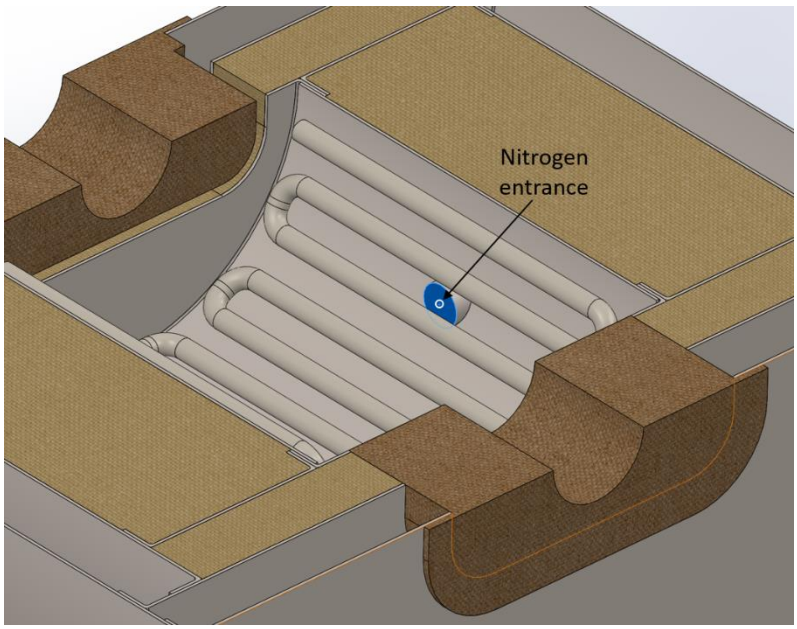

Figure 3.19 - Nitrogen entrance in the fixed half chamber.

Table 3.7 - Properties of the 68 series Alcon cryogenic solenoid valve (alcon, 2017).

Coil voltage DC	12, 24, 110 V
Coil voltage AC	24, 110, 120, 230 V
Pipe size	3/8''
Volume flow	3.0 m^3/h
Orifice size	16 mm

The simulations for the cooling process are then represented in the Figure 3.20 and Figure 3.21. As we can see the temperatures at the exterior surfaces are very close to the suitable operating temperature. They are just some degrees lower because these simulations are for the lowest temperature that adhesives can go with the cryogenic valve always opened (adhesive at -110 to -120 degrees). At the openings, the temperature is too low, but this is a localized temperature, because some millimeters away, the temperature has again a safe value.

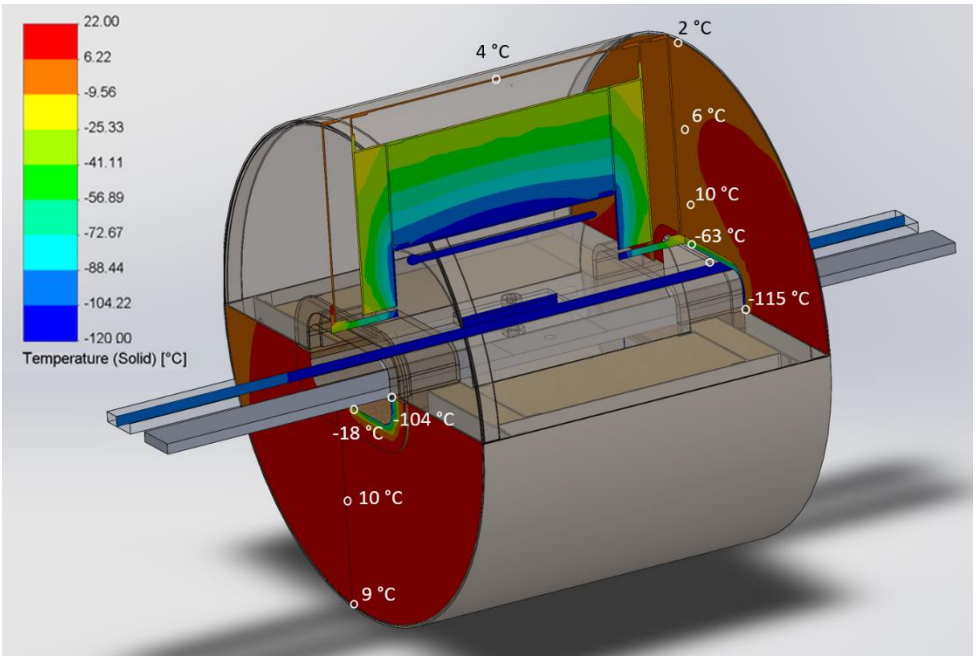

Figure 3.20 - Simulation in the *Tg* machine of the third design of the chamber for the cooling process.

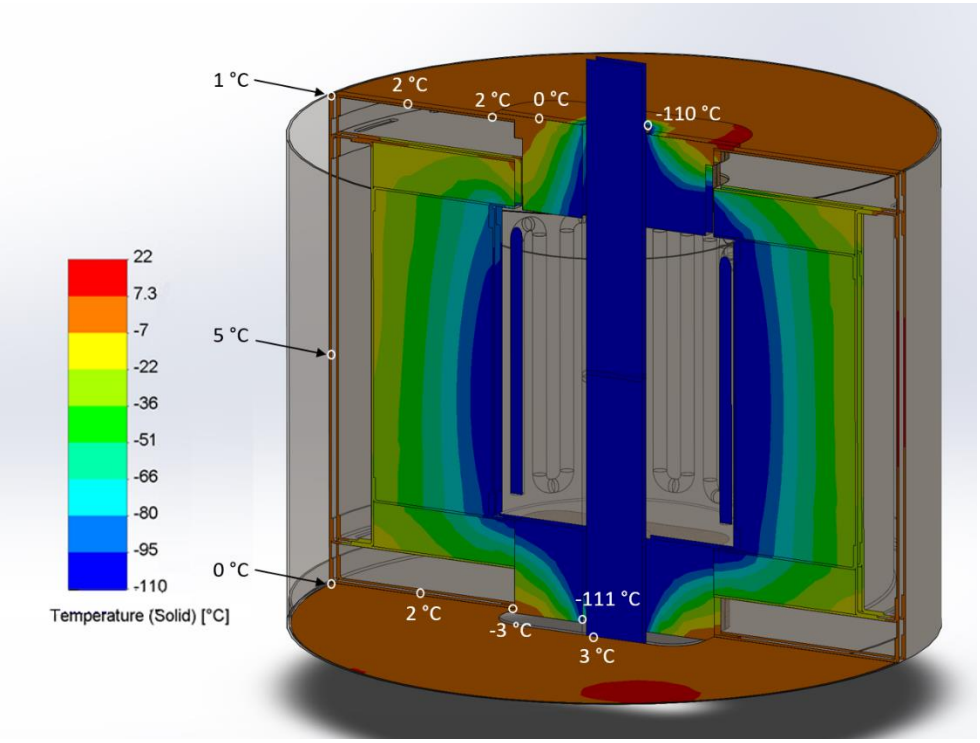

Figure 3.21 - Simulation in the torsion machine of the third design of the chamber for the cooling process.

To have an idea of how the mesh is defined in this software, an example will be exposed about the cooling process for the *Tg* machine. As shown in Figure 3.22, the cells of the mesh become more refined in the chamber and closer to it. The dimensions of the cells are represented in Figure 3.23.

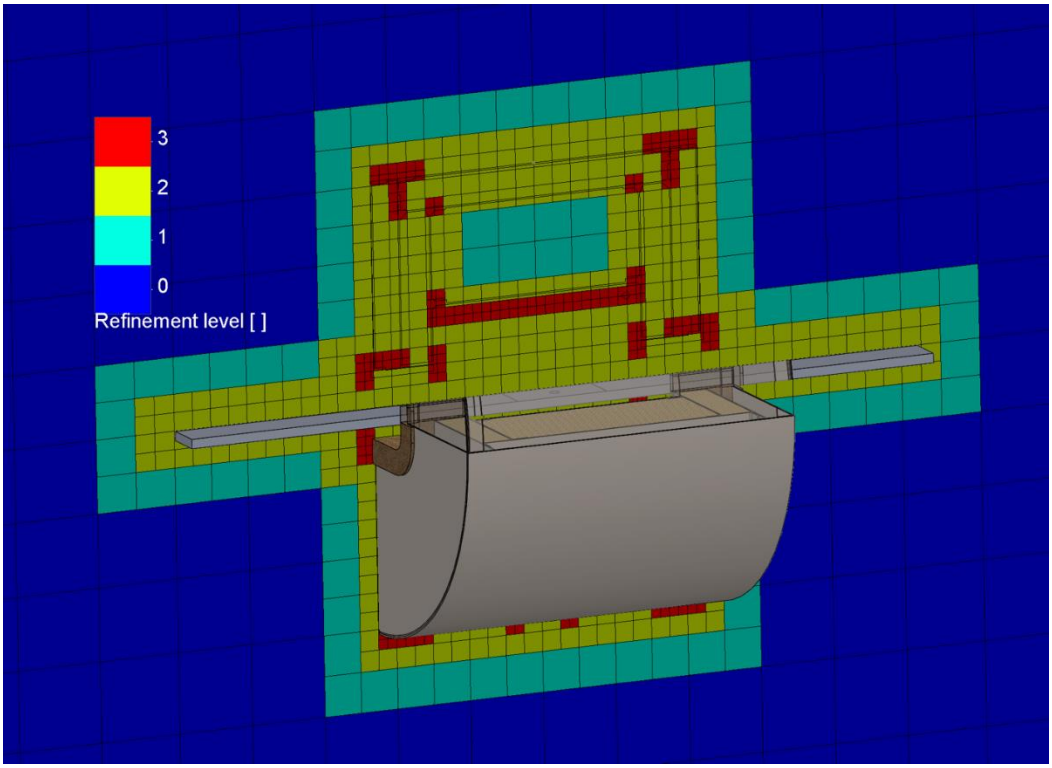

Figure 3.22 - Level of refinement of the mesh for a cooling test in the *Tg* machine.

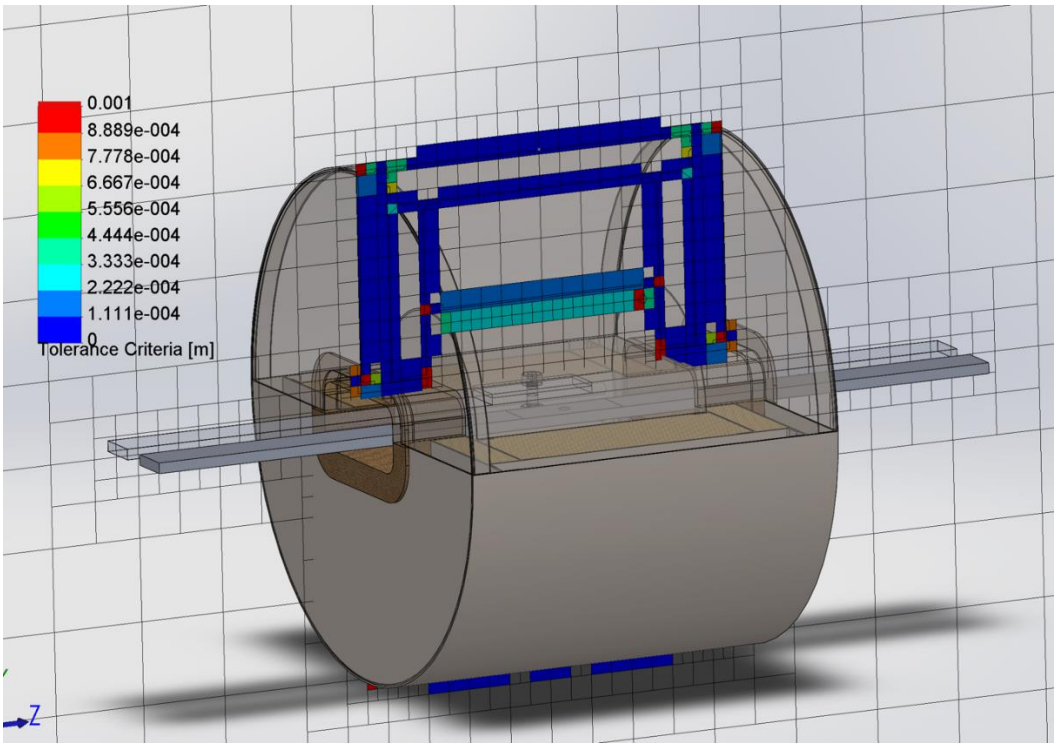

Figure 3.23 - Dimensions of the mesh for a cooling test in the *Tg* machine.

3.6 Adhesive temperature analysis in *Tg* machine and test duration

For the *Tg* machine, it is important to make a focused analysis of the adhesive temperature distribution because for this machine the heating/cooling process must be fast and at the same time the adhesive temperature gradient must be as low as possible.

Firstly, the analysis was made for the heating process and only after this analysis is done, analysis for the cooling process will be made. Several transient thermal simulations were made and the best case scenario for the temperature distribution is represented in the Figure 3.24 and Figure 3.25. The gradient temperature of the adhesive on this simulation is 32 °C, the test duration 13 min and the heating rate 14 °C/min.

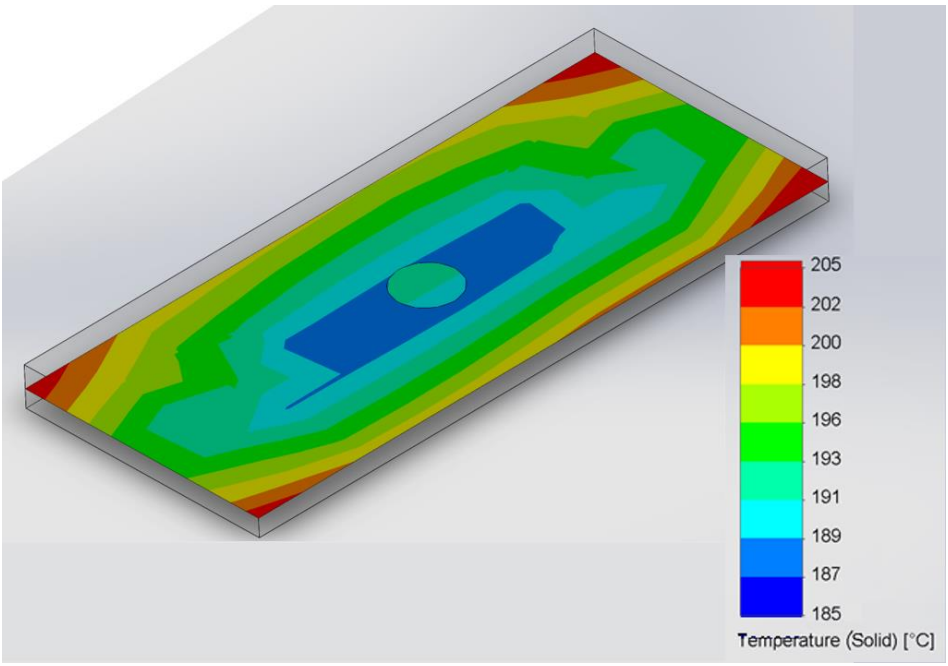

Figure 3.24 - Temperature distribution of adhesive for the *Tg* heating process for an aluminum specimen.

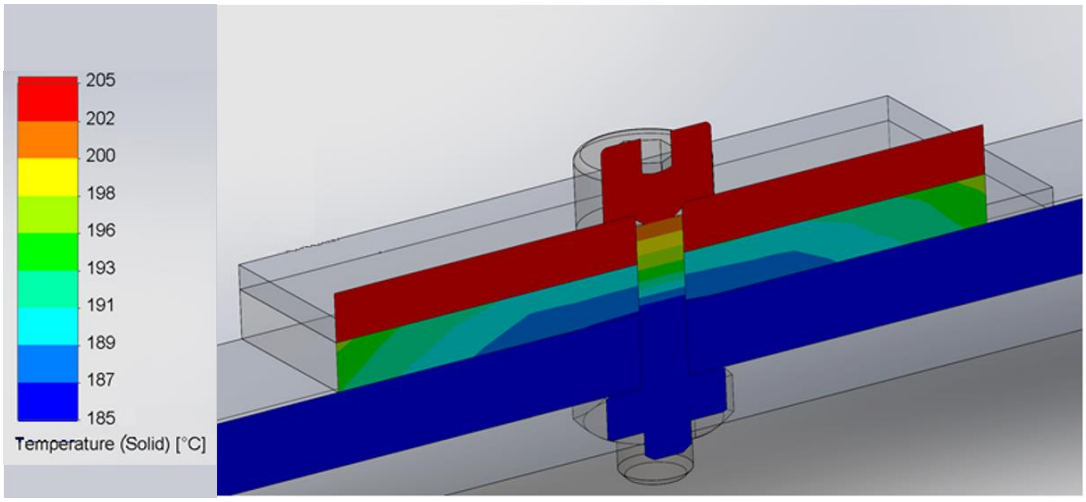

Figure 3.25 - Another perspective of the temperature distribution of adhesive for the *Tg* heating process for an aluminum specimen.

This distribution of temperature in the adhesive is not enough for the determination of the glass transition temperature of adhesives. So, it is necessary to find a solution to improve the temperature gradient. The fact that the temperature distribution in the adhesive is so high is because the specimen is made of aluminum. Aluminum is a material with a high thermal conductivity, and so, the heat will escape easily to the exterior through the specimen, instead of heating the adhesive sample. The solution that was taken to solve this problem was replacing the aluminum specimen for a stainless steel one. Because stainless steel has a much lower thermal conductivity than aluminum, heat should escape slower and adhesive temperature distribution should the smaller.

Several simulations were made and, in reality, changing the specimens to stainless steel improved significantly the distribution of temperatures in the adhesive and its gradient. In Table 3.8 are represented the temperature gradient of the adhesive for the aluminum and for the stainless steel specimens, with various heating velocities, so that we can easily verify that the stainless steel is a better choice for the specimens.

Table 3.8 - Minimum, maximum and gradient temperature in adhesive for different specimen materials.

Power	Material	Min Temp	Max Temp	Gradient	Heating rate
150+150 W	Aluminum	132 °C	251 °C	119 °C	75 °C/min
	Stainless steel	153 °C	240 °C	87 °C	81 °C/min
50+50 W	Aluminum	172 °C	204 °C	32 °C	14 °C/min
	Stainless steel	197 °C	208 °C	11 °C	15 °C/min

The best gradient temperature distribution that was obtained from simulations is 11 °C. This is for a heating rate of 15 °C/min and a test duration of 12 minutes. The evolution of the average temperature of the adhesive through time in the *Tg* machine is represented in the graph of the Figure 3.26, and the distribution temperature diagrams are represented in Figure 3.27 and Figure 3.28.

If we want a faster heating process, then the temperature gradient in the adhesive increases considerable, and if we improve the temperature gradient, the heating process takes too long to complete. So, this was the best compromise that could be achieved.

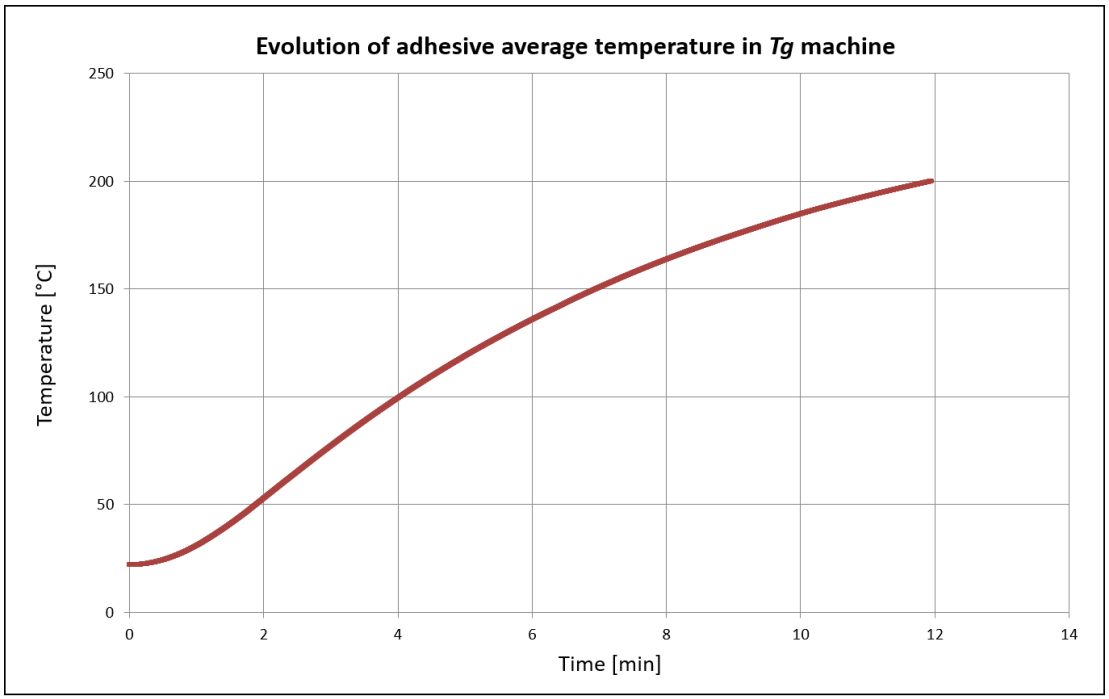

Figure 3.26 - Graph of the evolution of the adhesive average temperature in *Tg* machine for a heating process for a 50+50 W power.

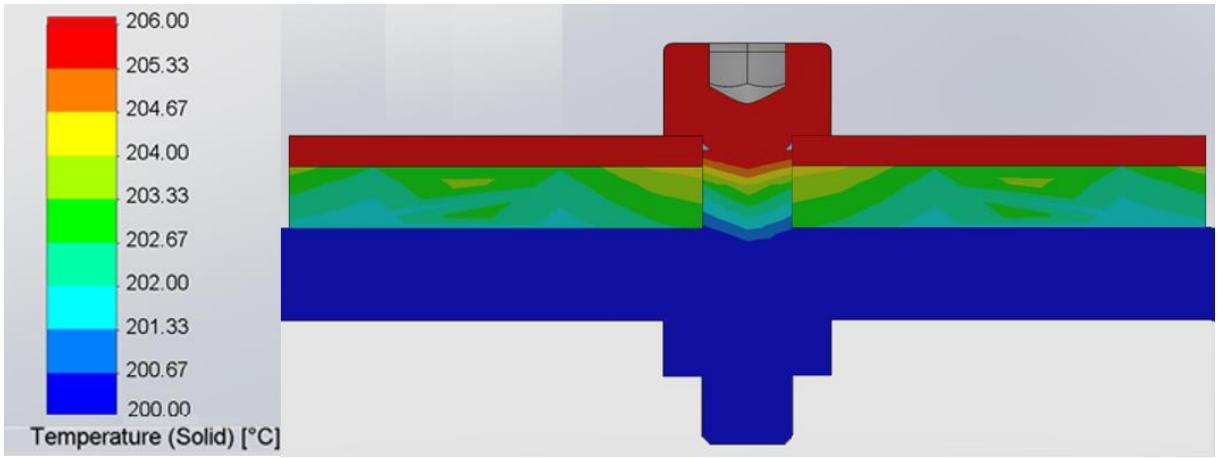

Figure 3.27 - Temperature distribution of adhesive for the *Tg* heating process for a stainless steel specimen.

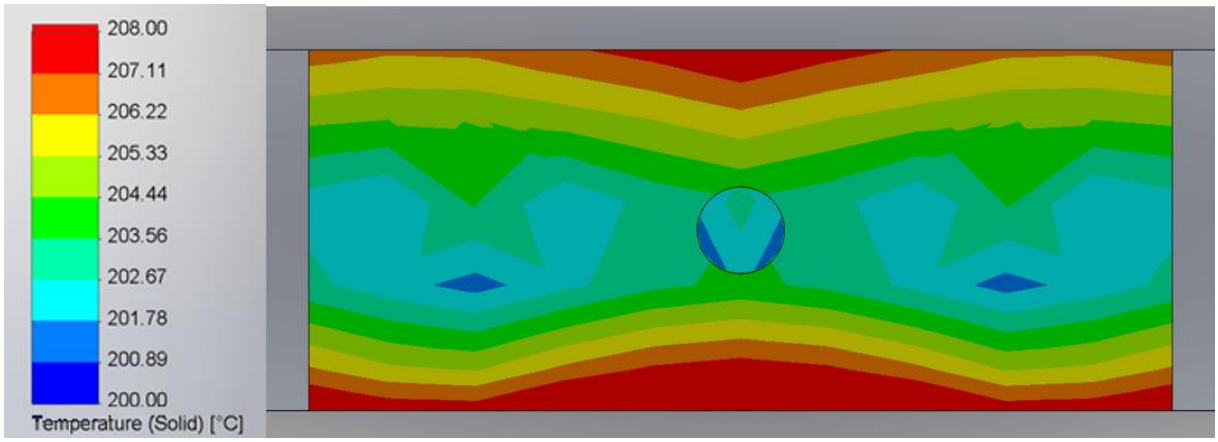

Figure 3.28 - Another perspective of the temperature distribution of adhesive for the *Tg* heating process for a stainless steel specimen.

Now, it is necessary to observe the temperature evolution of the adhesive along time, the test duration, and the gradient temperature of the adhesive for a cooling process. The transient simulation for the cooling process was done just for one case, namely the fastest cooling test possible. Only this simulation was performed because the solenoid valve works by being closed more time or opened more time according to the desired cooling rate, but in the SolidWorks software, we cannot define a transient inlet volume flow. So, only a simulation that considers the valve always opened was done. The minimum temperature for this process is -106 °C. The maximum temperature -98 °C, and the gradient temperature is 8 °C. The temperature distribution color diagrams are represented in Figure 3.29 and Figure 3.30. The cooling rate of this process is 40 °C/min and the test duration is 3 minutes.

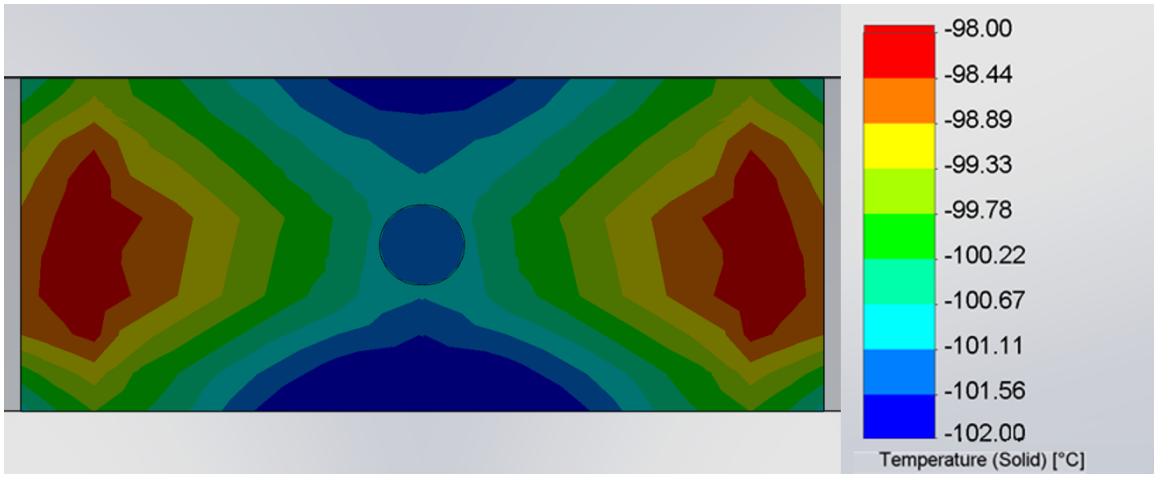

Figure 3.29 - Temperature distribution of adhesive for the *Tg* heating process for a stainless steel specimen.

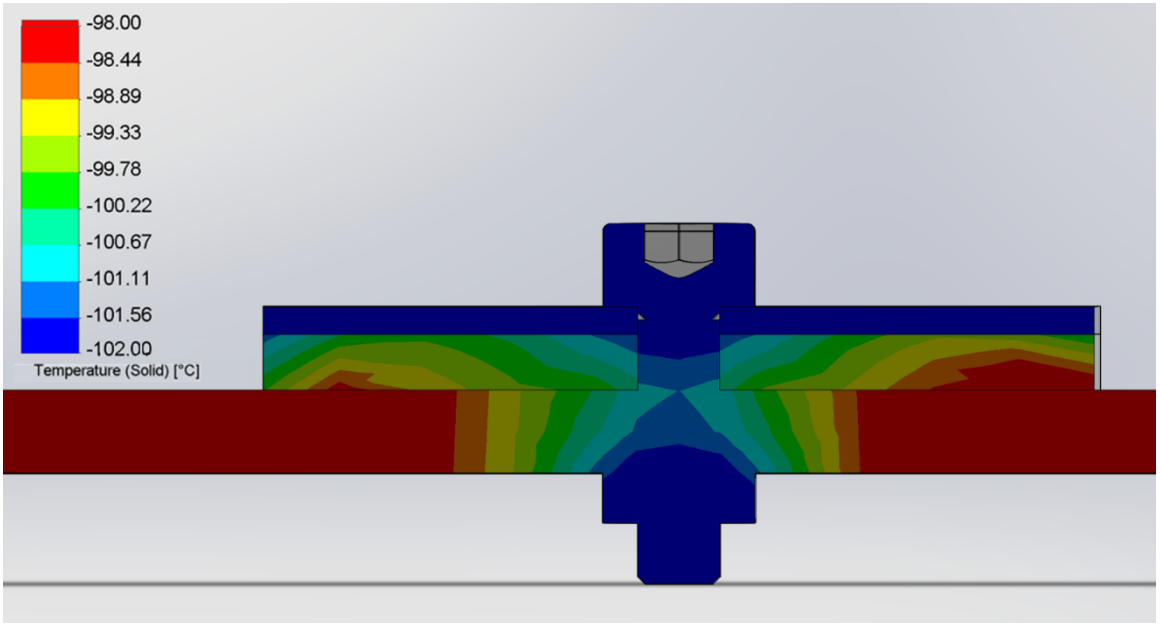

Figure 3.30 - Another perspective of the temperature distribution of adhesive for the *Tg* heating process for a stainless steel specimen.

The evolution of the average temperature of the adhesive through time in the *Tg* machine is represented in the graph of the Figure 3.31.

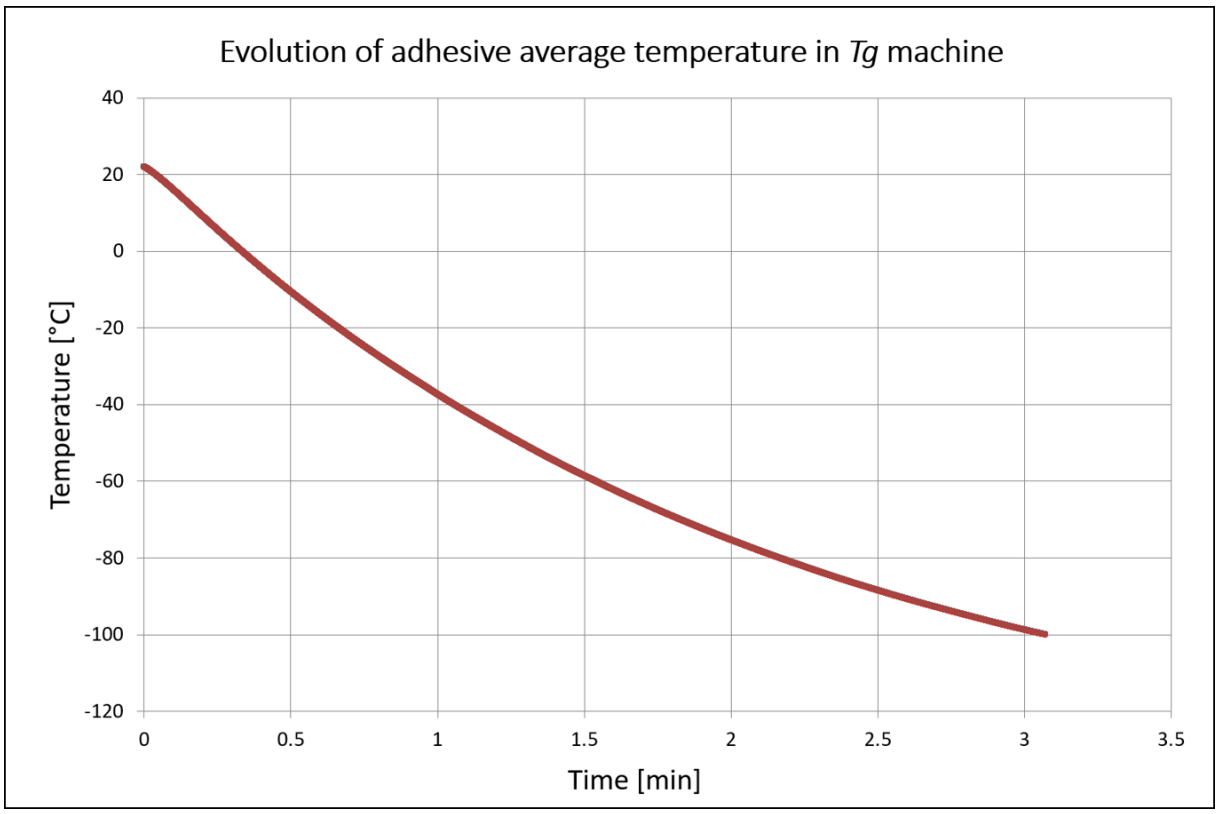

Figure 3.31 - Graph of the evolution of the adhesive average temperature in *Tg* machine for a cooling process.

3.7 Conclusions

In this chapter, the thermal chamber design was done, and validated with thermal and flow simulations. To homogenize the interior of the chamber, and maintain the temperature of the exterior wall at a reasonable value, a fan was required to blow air to the exterior air conduit.

In the *Tg* machine, the thermal chamber developed achieves a fast performance with a homogenous temperature in the adhesive. In the heating process, the chamber can heat from the ambient temperature up to 200 °C in 12 minutes, with a temperature gradient in the adhesive of 11 °C. For the cooling process, the chamber can cool from the ambient temperature down to -100 °C in 3 minutes, with a temperature gradient of 8 °C.

In the torsion machine, the chamber is also capable of testing the adhesive at a homogeneous temperature. In this machine, no temperature versus time simulation was done, since it is not required a fast heating in this test.

4 Automation project

In this chapter, the automation project of the thermal chamber will be presented. Firstly, the controller will be chosen, based on the temperature requirements. Secondly, all the electronic components required for the operation of the chamber will be presented. Before choosing the controller and other components, general considerations about temperature control and controller configuration will be analyzed.

4.1 Temperature control

A system designed to control temperature is primarily constituted of a temperature controller. A temperature controller is a device that controls any cooling/heating equipment. This control is done by comparing the desired set point with the actual temperature value that a sensor is measuring. The sensor is an element that converts temperature into an electric signal. After comparison, the error signal is processed and a control action is sent to the controllable components or some interface system (OMRON, 2007).

The temperature sensor can be:

- Thermocouple;
- Platinum resistance thermometer;
- Thermistor;
- Infrared non-contact sensor.

The interface hardware that is between the temperature controller and the heating/cooling elements can be:

- Solid state relay (SSR);
- Cycle controller;
- Power controller.

In Figure 4.1 is represented a scheme of a typical temperature control system and its main components, in this case, a heating system.

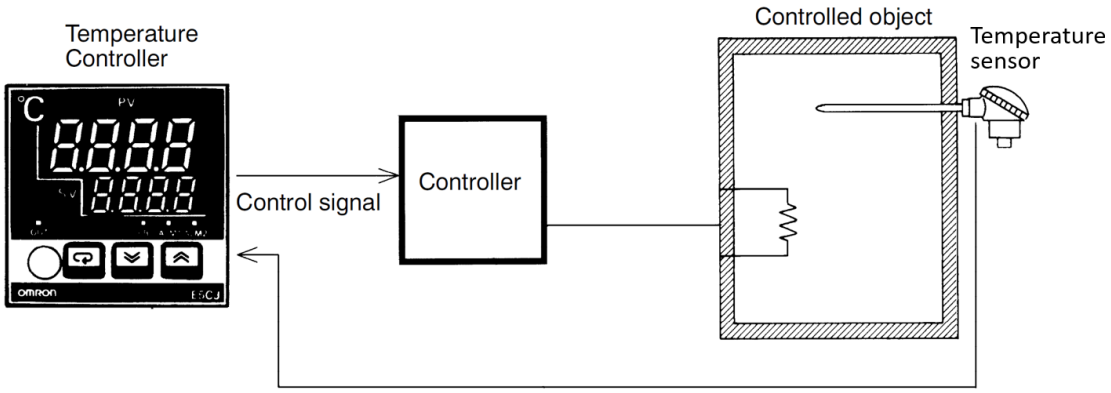

Figure 4.1 - Scheme of the typical components of a temperature control system (OMRON, 2007).

The temperature set point is defined in the temperature controller, but the response of the real temperature can have several behaviors, as seen in Figure 4.2. The temperature response can differ according to the characteristics of the controlled object and according to the control method of the temperature controller and controller parameters. In the graph (1) is represented the temperature response with overshoot, due to shortening too much the response time. When we try to eliminate the overshoot in the response, we need to increase the response time, but we need to take care so that the set point is not reached too slow, graph (3). In graph (2) is represented a good response, that corresponds to the quickest way that the set point is reached without occurring an overshoot.

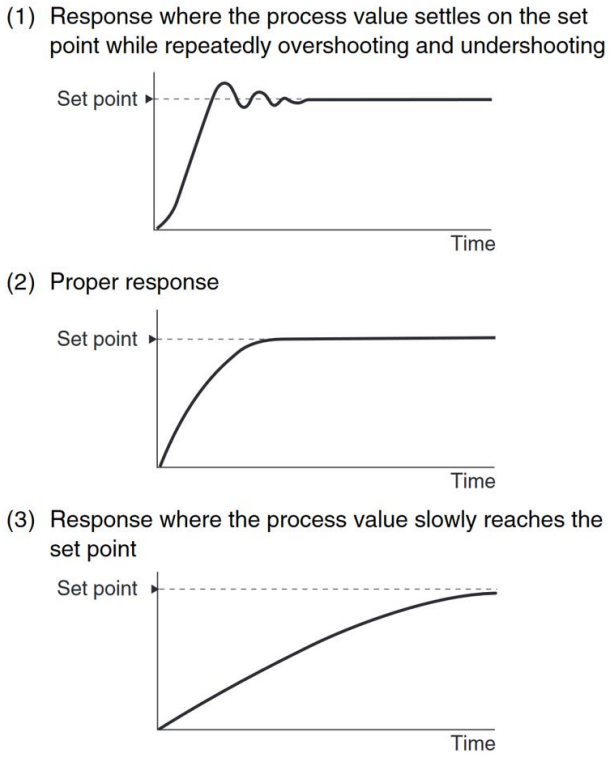

Figure 4.2 - Types of temperature control responses (OMRON, 2007).

4.2 Control methods

There are two main types of control action. One is the ON/OFF control and the other is the PID control. In the PID control, several types of controllers can exist, being all based on the three basic types of action, the proportional, the integral and the derivative.

4.2.1 ON/OFF control action

This is a simple type of controller, and so it is the control action that is present in the cheapest controllers. The principle is basically turning ON the control signal in the case that the measurable variable is lower than the required set point, and turning OFF the control action in the case that the measurable variable is higher than the required set point. The behavior of this type of control is represented in the graphs of Figure 4.3 (OMRON, 2007).

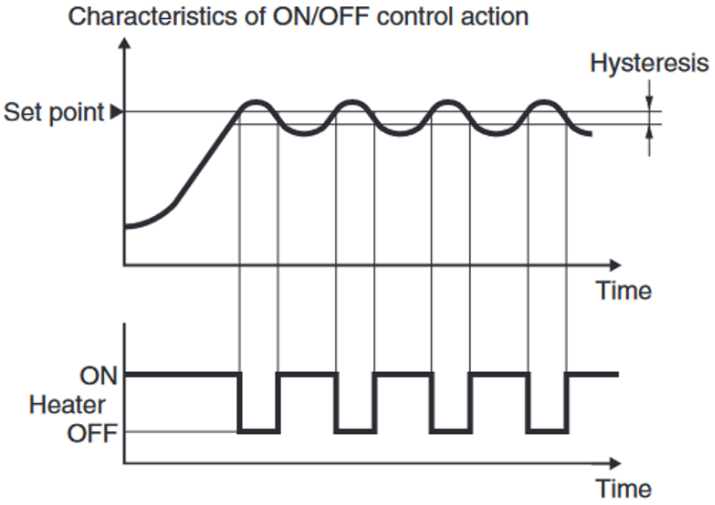

Figure 4.3 - Response behavior and control signal value of an ON/OFF control action (OMRON, 2007).

4.2.2 Proportional control action (P action)

The ON/OFF control action does not have a smooth behavior, so if we want to have a better behavior then we need to have a slower rate when approaching the set point. The proportional control action is then a solution, being basically an amplifier with a variable gain. This proportional relation is given by the proportional gain (K_p) (Ogata, 2010).

But the controller output signal has limitations, or even the corresponding actuator has limitations. For instance, a valve cannot be more opened than when it is fully opened, or cannot be more closed than when it is fully closed. So, it is necessary to define the 0 % and the 100 % control output action. Between the 0 % and the 100 % output action the relation between the input error and the output error is the proportional gain, Figure 4.4 (OMRON, 2007).

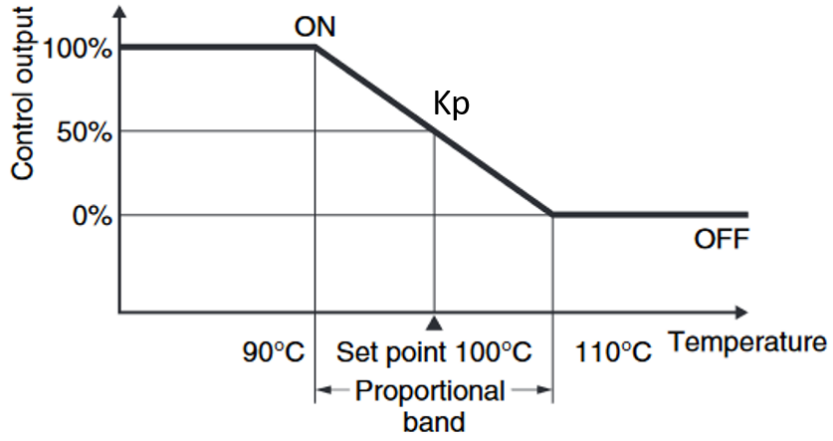

Figure 4.4 - Representation of the proportional gain for 100 °C set point (OMRON, 2007).

When choosing the proportional band, or gain, it is important to take some precautions because narrowing too much the proportional band, or increasing too much the proportional gain, will lead to instability of the systems (Ogata, 2010).

In a controller with just a proportional control action, there may be a steady-state error.

4.2.3 Integral control action (I action)

In a controller with an integral control action, the output control signal is changed at a constant rate, proportional to the input error. The integral control action is never used alone, we need to at least associate it with a proportional control action. To eliminate the steady-state error that may occur in a proportional controller, and obtain a response equal to the set point, then a proportional and integral control action are combined, as shown in Figure 4.5 (Ogata, 2010).

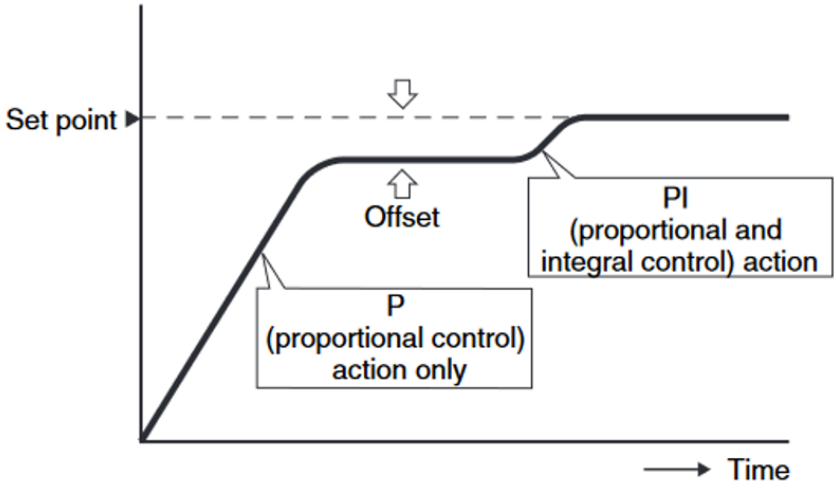

Figure 4.5 - Difference between a P controller and a PI controller (OMRON, 2007).

4.2.4 Derivative control action (D action)

In a controller with a derivative control action, the output control signal in proportion to the time derivative of the input error. The proportional and integral actions correct the control results, therefore the response to external disturbances will be slow. The derivative control action corrects the result of the control by adding the control output in proportion to the slope of temperature, so the response to an external disturbance will be much faster than in proportional and integral control actions, Figure 4.6. This is an important property when controlling temperature systems (Ogata, 2010, OMRON, 2007).

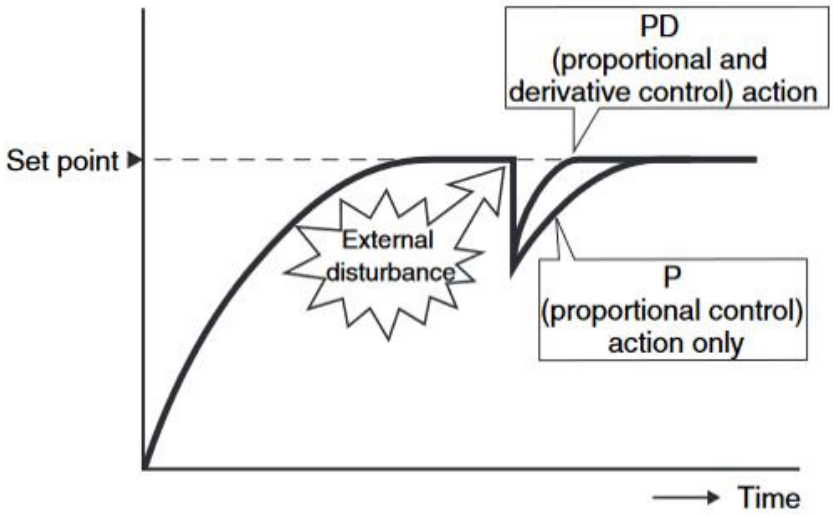

Figure 4.6 - Difference between a P controller and a PD controller when an external disturbance is applied (OMRON, 2007).

4.2.5 PID control

The controller with a PID control has the three control actions previously mentioned. In this type of controller, the advantages of each control action are joint together. The proportional action allows a smooth control, the integral action allows a zero steady state error, and the derivative action leads to a fast response to external disturbances.

4.3 OMRON temperature controllers

OMRON has a wide range of controllers specialized for temperature control. Because of that and because OMRON has a department nearby, the controller for the thermal chamber was selected from OMRON.

The OMRON controllers can operate with an ON/OFF control action or with whatever type of PID control we want (P, PI, PD, PID). These controllers are capable of a fuzzy control, estimating the temperature change and then making a fine adjustment of the control output.

Relay or solid state relay(SSR) outputs can only be ON (100 %) or OFF (0 %). However, a PID control outputs a control signal that varies from 0 to 100 %. Because of that, OMRON controllers use a method called time-proportioning control action that adds a time parameter (control period) to the output signal, to connect the 0 to 100 % output signal to the ON/OFF output state. For instance, if the control period is 2 s and the output signal is at 80 %, then the output state will be ON 1.6 s and OFF 0.4 s, as represented in Figure 4.7 (OMRON, 2007).

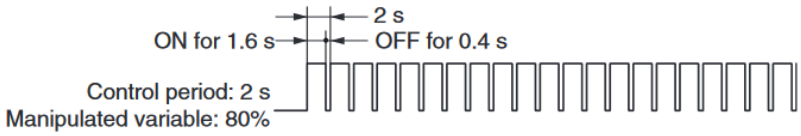

Figure 4.7 - Output state behavior for an 80 % output signal and a 2 s control period (OMRON, 2007).

For an accurate temperature control, the PID parameters need to be adjusted. This process of adjusting the PID parameters is called tuning. In OMRON controllers, the tuning can be manual or automatic. There are several types of methods to determine the PID parameters, being the step response method and the limit cycle method two typical methods.

4.3.1 Inputs of OMRON temperature controllers

The input of an OMRON controller can be of several types. It can be an analog current/voltage signal input or it can be a temperature sensor, more specifically a thermocouple, a platinum resistance thermometer or a thermistor.

Thermocouples have a cold and a hot junction, being the hot one the junction for temperature sensing and the cold one for measuring the signal, in this case being connected to the controller. The tables to determine an accurate value of the temperature with a thermocouple are for a cold junction at 0 °C, but the controllers are not at that temperature. Because of that, OMRON controllers are calibrated to a temperature between 20 and 25 °C, so that the temperature measuring can be accurate.

4.3.2 Outputs of OMRON temperature controllers

The outputs of an OMRON temperature controller can be of several types, as shown in Figure 4.8.

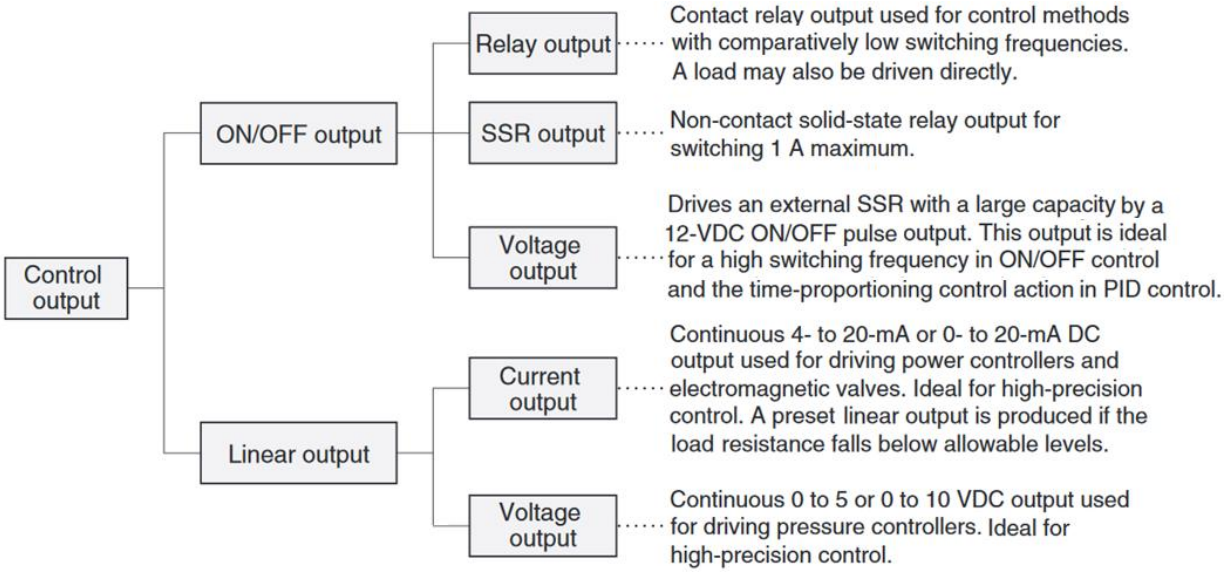

Figure 4.8 - Types of control outputs a temperature OMRON controller can have.

4.3.3 Definition of test profiles in OMRON temperature controllers

There are several methods to define the test profiles in OMRON temperature controllers. It is possible to define the test parameters (temperature set point and/or temperature change rate) manually on the controller. It is also possible to define the test profile and parameters from a computer by two methods: by an open serial communication protocol RS-485 or by a proprietary software of OMRON.

Because the RS-485 serial communication protocol is open, it is possible to do an interface for the computer based in C or VB, based on the RS-485 protocol norms.

The proprietary software of OMRON denominated CX-Thermo, together with the USB-Serial conversion cable of OMRON, makes it a plug and play solution, being an easier and more reliable solution. This is a more user-friendly solution than defining parameters directly in the controller, because it is easy to define all the segments of a profile, with a visual feedback.

4.4 Common precautions when using a solid state relay

Before applying a solid state relay (SSR), there are some considerations and precautions to take into account to prevent malfunction of the SSR either on the input or on the output circuit.

4.4.1 SSR input precautions

For the input circuit of a SSR, there can appear two types of noise, the pulse noise or the inductive noise.

The pulse noise appears when a pulse signal is applied to the input circuit of the SSR. To absorb this noise, a combination of a capacitor and a resistor are utilized. An example of that is represented in Figure 4.9, is the pulse signal done by a photocoupler (OMRON, 2017c).

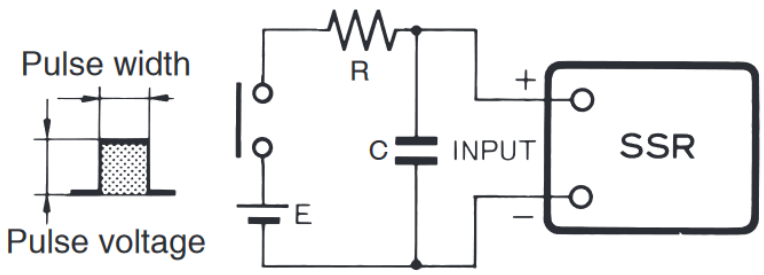

Figure 4.9 - Scheme of how to eliminate pulse noise in the input of a SSR with a photocoupler (OMRON, 2017c).

If the resistor has a too high value, the supply voltage (E) will not be able to satisfy the required input voltage of the solid state relay. Also, if the capacitor has a too high value, the release time will be too long, because the capacitor will take too much time to discharge (OMRON, 2017c).

The inductive noise can occur in the input of a solid state relay, which will cause the malfunction of the SSR. If the inductive noise that appears is electromagnetic noise, then it is required to use a twisted-pair wire. If the inductive noise that appears is static noise, then it is required to use a shielded cable (OMRON, 2017c).

4.4.2 SSR output precautions

For the output of the SSR, several types of noise can appear. The noise can be due the AC/DC switching surges. It is also required to take precautions about the inrush currents that can surge in the output of SSR due to the utilized loads.

AC switching SSR output noise surges

If a large voltage surge appears in the AC current applied to the SSR output, the resistor and capacitor snubber circuit built in the SSR may not be sufficient to suppress this surge, which may damage the SSR due to overvoltage (OMRON, 2017c).

In the OMRON solid state relays, there are some models that have a built-in varistor to absorb surge high voltages. These models are the G3NA, G3S, G3PA, G3NE, G3PH, G3DZ, G3RZ and G3FM.

In the case that the solid state relay does not have a built-in varistor to absorb surge high voltages, then it is required to add a varistor in the circuit.

DC switching SSR output noise surges

If an inductive load, such as a solenoid or an electromagnetic valve, is connected to the output of a solid state relay, then a counter electromotive force can occur. To prevent that, a diode placed in parallel with the load may be placed, Figure 4.10.

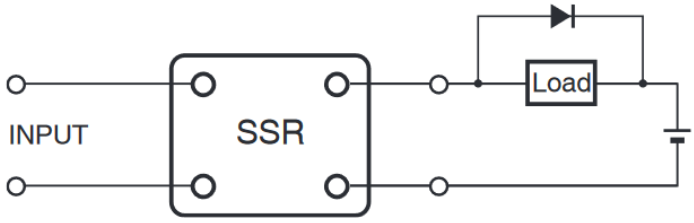

Figure 4.10 - Scheme of how to eliminate DC switching noise surges due to an inductive load in SSR output (OMRON, 2017c).

Inrush currents in SSR outputs

Depending on the type of load utilized in the output of the solid state relay, there will be different values of inrush current compared to the normal current. Approximate values for the inrush current and normal current ratio, for different loads, is presented in Figure 4.11.

Load	Solenoid	Incandescent lamp	Motor	Relay	Capacitor	Resistive load
Inrush current/ Normal current	Approx. 10 times	Approx. 10 to 15 times	Approx. 5 to 10 times	Approx. 2 to 3 times	Approx. 20 to 50 times	1
Waveform	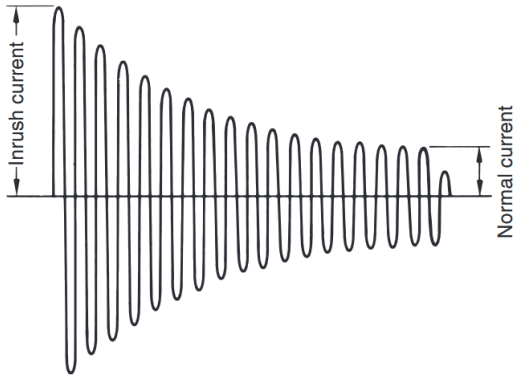					

Figure 4.11 - Ratio between inrush and normal current for different loads applied in SSR output (OMRON, 2017c).

If the load is a resistive one, then there will be no inrush current and so, no precautions are required.

If the load is a lamp or a motor, then the inrush current will exist and be considerably superior to the normal load so, it is required to choose a solid state relay with an inrush current resistance that is at least twice larger than the inrush current of the load.

If the load is one of small capacity, like a relay, even small, there is a leakage current from the load that can damage the solid state relay if its release current is smaller. If the SSR release current is smaller than the leakage current, then it is required to implement a bleeder resistance in parallel with the load.

If the load is a capacitor, then when the solid state relay is OFF, it will be subjected at the same time with the power supply voltage and the capacitor voltage. So, it is required to choose a SSR with an operating input voltage of twice the value of the power supply (OMRON, 2017c).

4.5 Electronic components

As mentioned before the thermal chamber needs to operate between the temperature of -100 and 200 °C. Because of that, it is required a cooling and a heating system. As said in section 3.5, the heating mechanism will be done by two spiral electric resistances and the cooling mechanism will be done by injecting liquid nitrogen using a cryogenic solenoid valve. To make the control of the system, a temperature controller of OMRON will be utilized. To power the electric resistances, a solid state relay will be utilized between the controller (Out1) and the resistances. To control the cryogenic solenoid valve, a relay control output in the controller will be utilized (Out2). To measure the temperature a thermocouple will be utilized, connected to the controller input. The required fan will be powered from a 5 VDC power supply. This fan will be connected to an auxiliary output of the controller in order to turn ON/OFF the fan when wanted. In Figure 4.12 is represented a diagram of all the electronic components for the thermal chamber.

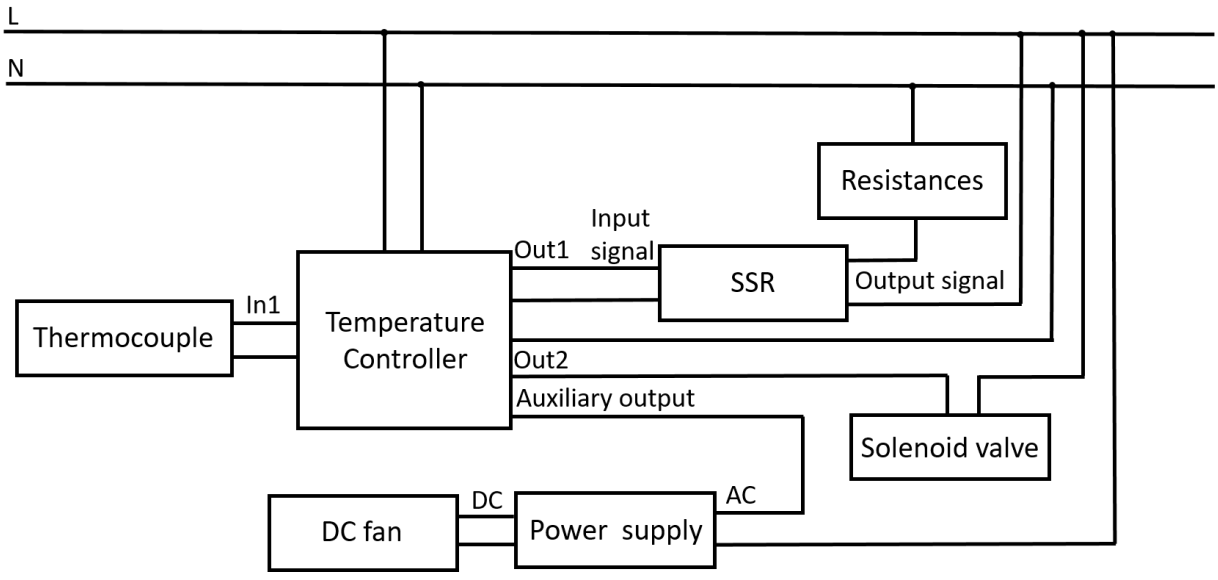

Figure 4.12 - Diagram of all the electronic components of the system.

4.5.1 Temperature controller

The requirements for the temperature controller are:

- One universal input for temperature sensor, in particular, an input for a thermocouple;
- One voltage control output for driving a solid state relay;
- One relay control output to control the cryogenic solenoid valve;
- One auxiliary relay output to control the fan;
- Ability to define step as well as ramp set points. The ramp set point is for the *Tg* test machine, to ensure a constant temperature rate during the test. The step set point is for the torsion machine;
- Compatible with a 230 VAC, 50 Hz power supply voltage.

The selected controller is the E5CC-TQX3A5M-000, Figure 4.13, from the E5CC-T OMRON series, because it complies with all the requirements of the system. This controller has a universal input to connect a thermocouple, a three-wire platinum resistance thermometer or an analog current/voltage signal. It has one output for driving SSR. It has also three auxiliary outputs, that are 100 to 240 VAC relays. One of the auxiliary relay outputs can operate as the second control output. This controller can be supplied with a power voltage input of 100 to 240 VAC. Finally, this controller was selected because it is possible to define a step, or a ramp set point, can be programmed with a profile of 32 segments, and defined the type of control output to be utilized in each segment. For instance, for the *Tg* machine, if we want to determine a *Tg* above the ambient temperature, then it is required a set point like the one represented in Figure 4.14. We need to control the output of the resistances in the heating process, and the output of the cryogenic solenoid valve in the cooling.

Figure 4.13 - E5CC-T OMRON temperature controller series (OMRON, 2017a).

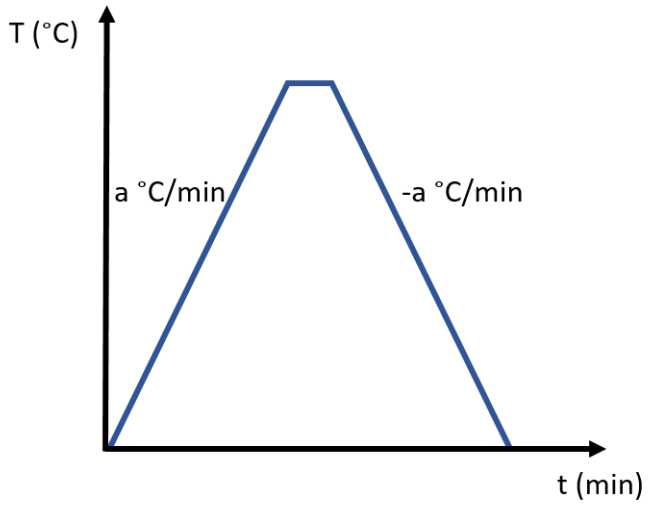

Figure 4.14 - Temperature profile to test a *Tg* above the ambient temperature of an adhesive.

The solution adopted for the definition of the temperature profiles is based on the proprietary software of OMRON, CX-Thermo. As said before, for communicating with the controller it is required a USB - serial communications conversion cable. Although this solution is more expensive, this is easier and more reliable.

4.5.2 Spiral thermal resistance

The required spiral thermal resistances were defined in section 3.3.

4.5.3 Solid state relay

The control output for driving the SSR is a voltage output of 12 VDC. The spiral resistances utilized operate at the 230 VAC monophasic power, Table 3.3. Considering these, it is required a solid stat relay with an input operating voltage range that covers the 12 VDC and an output voltage range that covers the 230 VAC. It is also required that the load current that the SSR can have through its output terminals is larger than the current required to load the two electric resistances. The resistances will be placed in parallel so that the overall heat power they generate is 400 W. The current required to load the resistance is 1.74 A, Figure 4.15.

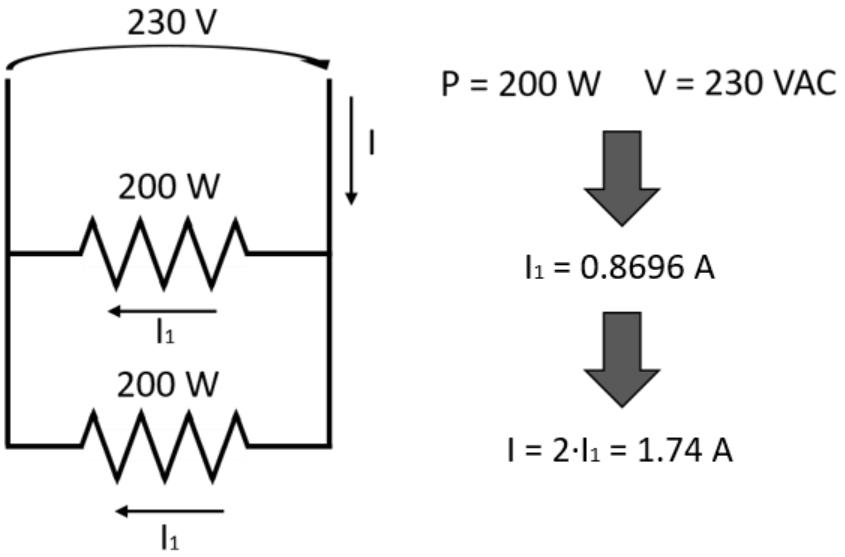

Figure 4.15 - Scheme of how many current is required to load the resistances.

The selected solid state relay is the G3NA-205B-UTU from OMRON G3NA series, Figure 4.16. The input operating voltage range is from 5 to 24 VDC and the load voltage range is from 24 to 240 VAC. The load current range is 0.1 to 3 A without a heat sink, so all requirements are fulfilled.

Figure 4.16 - OMRON solid state relay from G3NA series (OMRON, 2017b).

Regarding the solid state relay precautions pointed in chapter 4.4, for the input no additional equipment is required because the switching signal is a DC one. For the output, no precautions are required for the AC current switching surges, because the G3NA SSR has a built-in surge absorbing varistor. No additional precautions are required due to inrush current because no inrush current appears in resistive loads.

4.5.4 Cryogenic solenoid valve and cryogenic safety valve

The cryogenic solenoid valve utilized has yet been defined in section 3.5. Normally, in cryogenic cooling systems, a cryogenic safety valve is utilized for protection against thermal expansion in pipeworks. It was selected an HEROSE cryogenic safety valve, type 06002, with a pipe size of 3/8'', Figure 4.17.

Figure 4.17 - HEROSE cryogenic safety valve type 06002 (HEROSE, 2017).

4.5.5 DC fan

The DC fan utilized to generate an inlet air flow in the external conduit of the chamber has yet been defined in section 3.5.

4.5.6 Power supply

Because the DC fan has an operating 5 VDC power, then a power supply is required to convert the 230 VAC to the 5 VDC. The selected power supply is the LD02-10B05 from the brand RS Pro, Figure 4.18. The characteristics of this power supply are presented in Table 4.1.

Figure 4.18 - RS Pro LD02-10B05 power supply (RS, 2017b).

Table 4.1 - Characteristics of RS Pro LD02-10B05 power supply (RS, 2017b).

Output voltage	5 VDC
Output current	400 mA
Input voltage	85 - 305 VAC or 120 - 430 VDC
Power rating	2 W

4.5.7 Thermocouple

The thermal chamber is projected to operate between the temperature range of -100 to 200 °C. So, a type T thermocouple was selected because this type of thermocouples is suited for temperature in the -200 to 350 °C range. The selected thermocouple is the RS Pro, type T, with a RS code 621-2209, Figure 4.19. This thermocouple has a two meters cable reinforced with a glass fiber sleeve.

Figure 4.19 - RS Pro 621-2209 type T thermocouple (Pro, 2017a).

4.5.8 Power switch

To isolate the mains power from the system, a power switch is required. This has safety reasons so that the mains power is only connected to the system when the operator wants. The selected power supply is a 3 pole non-fused one from Allen Bradley, with the reference number 194E-E16-1753-4N, Figure 4.20. The characteristics of this power switch are presented in Table 4.2.

Figure 4.20 - Allen Bradley 3 pole non-fused power switch with reference number 194E-E16-1753-4N (Bradley, 2017).

Table 4.2 - Characteristics of Allen Bradley 3 pole non-fused power switch with reference number 194E-E16-1753-4N (Bradley, 2017).

Number of poles	3
Maximum current	16 A
Voltage rating	690 VAC
Power rating	73.5 kW

4.5.9 Indicator light

To know if the mains power is connected to the system an indicator light is required. The selected one is a green LED from RS Pro, with a reference number 207-242, Figure 4.21. This indicator green LED has a voltage rating of 230 VAC.

Figure 4.21 - RS Pro green indicator LED with reference number 207-242 (Pro, 2017b).

4.6 Electrical circuit

Now that all electronic components are selected, it is possible to do the electric circuit of all the system. For that, the SEE Electrical V5 software was utilized. The electric circuit of the thermal chamber is represented in Figure 4.22.

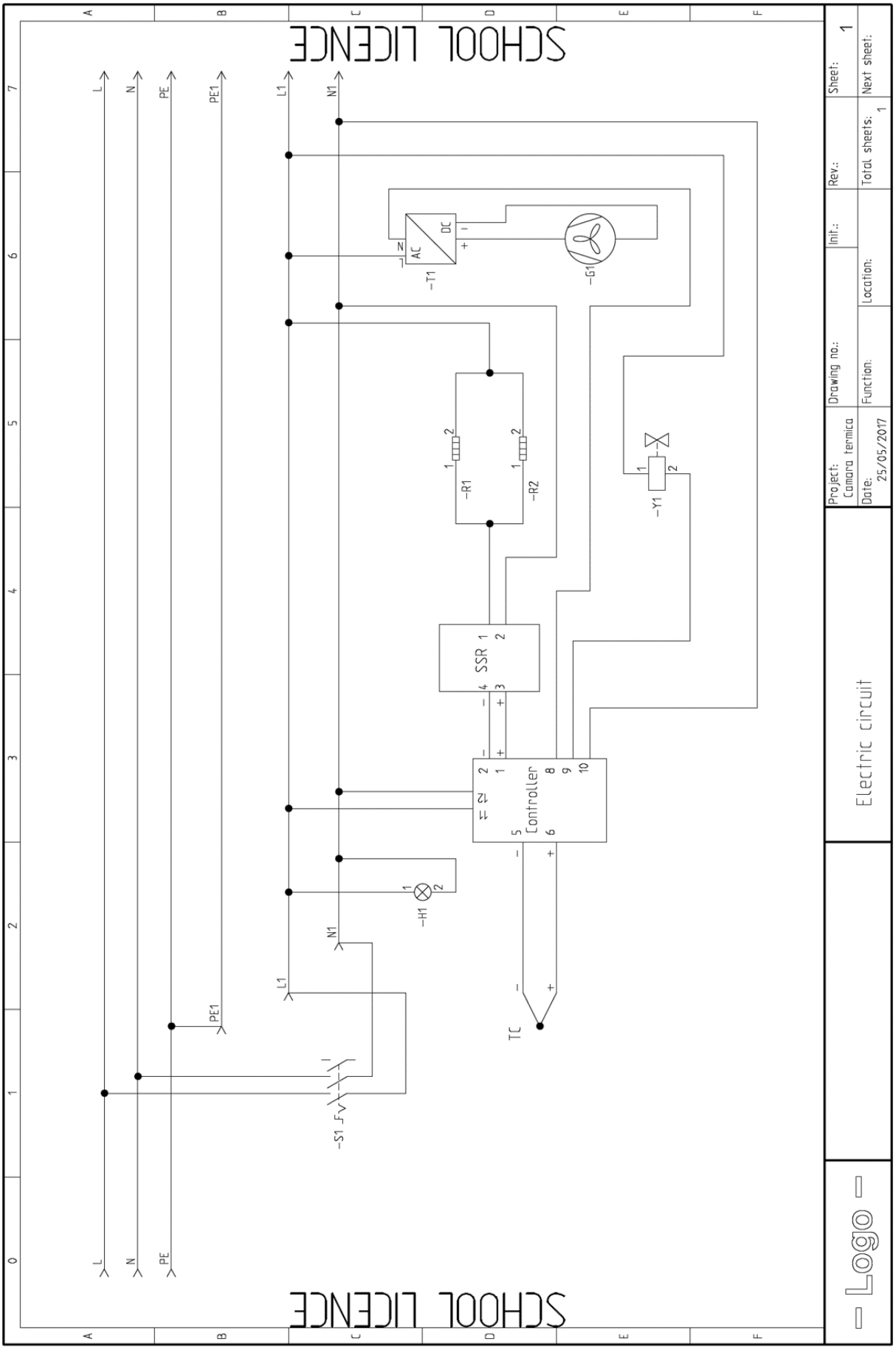

Figure 4.22 - Electric circuit of the thermal chamber.

5 Conclusions

The main objective of this dissertation consisted in the design of a portable thermal chamber for operating in the temperature range of -100 to 200 °C, for two machines: the glass transition temperature machine and the torsion machine. The work included the mechanical, the thermal, and the automation project of the chamber.

The first stage consisted on a literature review, to understand well how the two machines work, and the requirements of the thermal chamber. The literature review was also relevant to know typical existing thermal chambers, and the type of cooling/heating systems that are used. From this review, it was concluded that the thermal chamber needs to have a fast heating/cooling rate so that the *Tg* can be determined the most accurately possible. Is was also concluded that the structure of the chambers is normally made of a sandwich structure. The best solution for the heating process is using thermal resistances and, for the cooling process, liquid nitrogen.

The second stage of this project consisted on the thermal chamber design. Here several iterations were done until the final system. To validate the thermal chamber design, thermal and flow simulations were done with SolidWorks software. It was concluded that to comply with the dimensional limitations of the chamber, it is required a fan for creating a constant inlet flow of air at ambient temperature to the exterior air conduit of the chamber. This fan has the objective of maintaining the temperature of the exterior walls at a reasonable value, for user protection. Because the airflow generated by the fan is redirected to the chamber openings, it has also the role of preventing excessive heat transfer between the interior and the exterior of the chamber, and so maintain the interior atmosphere more homogenous. In the *Tg* machine, with the design developed, the thermal chamber can heat from the ambient temperature up to 200 °C in 12 minutes, with a temperature gradient in the adhesive of 11 °C. For the cooling process, the thermal chamber can cool from the ambient temperature down to -100 °C in 3 minutes, with a temperature gradient in the adhesive of 8 °C. In the torsion machine, the chamber is also capable of testing the adhesive at a homogeneous temperature. In this machine, the evolution of temperature along time simulation was not done, since it is not required a fast heating in this test.

In the last stage, the automation project was done. For that, all the electronic components were selected and the electric circuit was done. The components consisted of a thermocouple to measure the temperature, two spiral resistances to heat the chamber, a solid state relay connected to the resistances, a cryogenic solenoid valve to control the nitrogen flow, a fan to generate the air flow, and an industrial temperature controller to control all the system.

It is now in process with the “UP Inovação” department the registration of a patent to protect the thermal chamber designed in this thesis.

5.1 Future work

Future work includes the project of the structure that will hold the thermal chamber. Moreover, since the chamber is required to operate in both the horizontal and vertical direction, it is also required to design the mechanism that will allow the rotation of the chamber relative to the structure.

Also, the thermal chamber needs to be constructed, and then tests are necessary to validate the design.

6 References

alcon. 2017. "68 series solenoid calves." https://www.finecontrols.co.uk/image/data/manuals/Alcon%20datasheets/68%20series.pdf.

Bergman, T.L., e F.P. Incropera. 2011. *Fundamentals of Heat and Mass Transfer*: Wiley.

Bradley, Allen. 2017. "16 Amp At-Motor IEC Disconnect Switches." http://docs-europe.electrocomponents.com/webdocs/1415/0900766b8141577b.pdf.

da Silva, L.F.M., A. Öchsner, e R.D. Adams. 2011. *Handbook of Adhesion Technology*: Springer Berlin Heidelberg.

da Silva, Lucas Filipe Martins, Antonio Goncalves de Magalhaes, e Marcelo Francisco SF de Moura. 2007. *Juntas adesivas estruturais*: Publindustria.

Dallas, G., e S. Aubuchon. 2016. TA Instruments DSC Cooling Accessories. 109 Lukens Drive, New Castle, DE 19720, USA TA Instruments.

Daniel, Tufan Alexandru. 2013. "Development of a dynamic mechanical analysis with a vibrating beam method." Master Degree, Mechanical Engineering, Faculdade de Engenharia da Universidade do Porto.

Fibrosom. 2017. "Lâ de Rocha." http://www.fibrosom.com/.

Group, KANTHAL® - Part of Sandvik. 2017. "Heating Elements." http://www.kanthal.com/en/products/furnace-products-and-heating-systems/electric-heating-elements/.

Gunnarsen, Lars, Peter A. Nielsen, e Peder Wolkoff. 1994. "Design and Characterization of the CLIMPAQ, Chamber for Laboratory Investigations of Materials, Pollution and Air Quality*." *Indoor Air* 4 (1):56-62. doi: 10.1111/j.1600-0668.1994.t01-3-00007.x.

HEROSE. 2017. "Cryogenic." https://www.herose.com/eng/products/cryogenic-services/06002_06006_dt.php.

Hutchinson, John M. 2009. "Determination of the glass transition temperature." *Journal of Thermal Analysis and Calorimetry* 98 (3):579. doi: 10.1007/s10973-009-0268-0.

Inc., Hyndman Industrial Products. 2017. "Coil & Heating Elements." http://resistancewire.com/products-services/coils-heating-elements/.

Instruments, TA. 2016. "Fixtures and Chambers." http://www.tainstruments.com/products/electroforce-mechanical-testers/electroforce-accessories-upgrades/fixtures-and-chambers/.

Kosmač, Alenka. 2013. "Adhesive Bonding of Stainless Steels." *Materials and Applications Series*, 20.

Lever, Trevor, Peter Haines, Jean Rouquerol, Edward L Charsley, Paul Van Eckeren, e Donald J Burlett. 2014. "ICTAC nomenclature of thermal analysis (IUPAC Recommendations 2014)." *Pure and Applied Chemistry* 86 (4):545-553.

Li, G., P. Lee-Sullivan, e R. W. Thring. 2000. "Determination of Activation Energy for Glass Transition of an Epoxy Adhesive Using Dynamic Mechanical Analysis." *Journal of Thermal Analysis and Calorimetry* 60 (2):377-390. doi: 10.1023/a:1010120921582.

Menczel, Joseph D, e R Bruce Prime. 2014. *Thermal analysis of polymers: fundamentals and applications*: John Wiley & Sons.

Ogata, K. 2010. *Modern Control Engineering*: Prentice Hall.

OMRON. 2007. Technical Explanation for Temperature Controllers.

OMRON. 2017a. "E5_C / E5_C-T datasheet." https://assets.omron.eu/downloads/datasheet/en/h177_e5_c_e5_c-t_datasheet_en.pdf.

OMRON. 2017b. "Solid State Relays - G3NA." https://assets.omron.eu/downloads/datasheet/en/j166_g3na_datasheet_en.pdf.

OMRON. 2017c. Solid State Relays Common Precautions.

Portugal, RELACRE - Associação de Laboratórios Acreditados de. 2004. Guia RELACRE 19.

Pro, RS. 2017a. "Data sheet cable thermocouple." http://docs-europe.electrocomponents.com/webdocs/157a/0900766b8157a82c.pdf.

Pro, RS. 2017b. "RS Pro Prominent Indicator Panel Mount, 22mm Mounting Hole Size, Green LED, Tab Termination, 16 mm Lamp Size, 230 V ac." http://docs-europe.electrocomponents.com/webdocs/1578/0900766b81578e1b.pdf.

RS. 2017a. "Components." http://pt.rs-online.com/web/.

RS. 2017b. "datasheet LD01 & LD02 SERIES." http://docs-europe.electrocomponents.com/webdocs/1587/0900766b8158799e.pdf.

saidacasca. 2017. "Resistência espiral (mola) 200W." http://www.saidacasca.com/incubacao/acessorios-incubacao/pecas-incubadoras/resistencia-espiral-_mola_-200w.

SIGMA. 2000. "Cryogenic Cooling for Temperature Chambers and Thermal Platforms." http://www.intestthermal.com/pdfs/Thermal_ds/Cryogenic_Cooling_Explained.pdf.

Telha, Rui Mário Tavares. 2012. "Development of a dynamic mechanical analysis with a vibrating beam method to determine the glass transition temperature (Tg) of adhesives."

Zarr, R.R., D.M. Burch, e A.H. Fanney. 1995. *Heat and Moisture Transfer in Wood-Based Wall Construction*: DIANE Publishing Company.

Zhang, Y., R. D. Adams, e Lucas F. M. da Silva. 2013. "A Rapid Method of Measuring the Glass Transition Temperature Using a Novel Dynamic Mechanical Analysis Method." *The Journal of Adhesion* 89 (10):785-806. doi: 10.1080/00218464.2013.763677.